

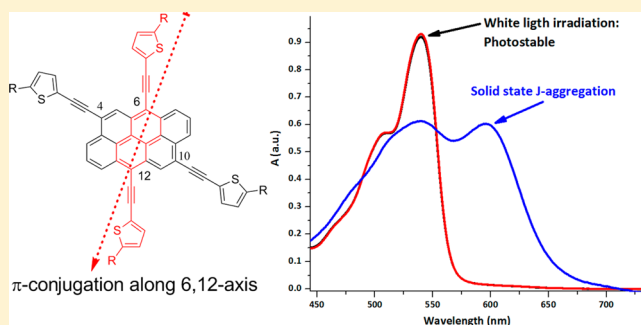
Cruciform Alkynylated Anthanthrene Derivatives: A Structure–Properties Relationship Case Study

Jean-Benoît Giguère, Joël Boismenu-Lavoie, and Jean-François Morin*

Département de Chimie and Centre de Recherche sur les Matériaux Avancés (CERMA), Université Laval, 1045 Ave de la Médecine, Québec, Canada G1V 0A6

Supporting Information

ABSTRACT: An efficient and versatile synthetic strategy toward cruciform anthanthrene compounds using Sonogashira couplings steps was developed. Acetylenic linkers were used to effectively extend the π -conjugation of polycyclic anthanthrene and anthanthrene compounds and tune their optoelectronic properties. Structure–property relationships supported by DFT calculations indicated more effective π -conjugation along the 6,12 axis than along the 4,10 axis. These molecules displayed strong J-aggregation both in solution and in the solid state and proved to be highly photostable with reversible redox processes, which are properties of interest in materials sciences.



INTRODUCTION

The fascination of chemists for aromatic molecules has never weakened, from the earlier studies of aromaticity with Huckel's¹ and Clar's² rules to the more recent developments of semi-conducting π -conjugated molecules for organic electronics.^{3,4} Fused aromatic compounds, especially acenes, have attracted a lot of attention because of their performance as semiconductors in organic field-effect transistors (OFETs). Among others, pentacene and its derivatives such as TIPS-pentacene exhibit excellent charge-carrier properties, and mobilities of over $1 \text{ cm}^2 \text{ V}^{-1} \text{ s}^{-1}$ are routinely achieved under optimized conditions. Some limitations of acene derivatives are their poor photostability, sensitivity to oxidation, and rather complex synthesis.^{5,6} A strategy to tackle these obstacles that limit their use in organic electronics is precise control of the frontier molecular orbitals, namely, the highest occupied molecular orbital (HOMO) and lowest unoccupied molecular orbital (LUMO).⁷ The manipulation of the HOMO and LUMO energy levels is particularly important in organic photovoltaics (OPVs), in which the absorption of photons and the electron transfer between the donor and acceptor materials are governed by the positions of the frontier orbitals. For polycyclic aromatic molecules, primarily three strategies have been used to tune the optoelectronic properties: heteroatom (N, O, S, Se) replacement, core substitution (halogens, cyano), and side-chain engineering.^{5,8} Electron-withdrawing substituents such as fluoride and imines are often introduced to lower the HOMO and LUMO levels and, consequently, to improve the stability toward oxidation and reach an n-type or ambipolar character. At the opposite extreme, thienoacenes have been extensively used to obtain p-type mobility.

Relevant to the present work, the Choi group went in a different direction and used X-shaped anthracene derivatives as

active materials in both solar cells and OFET applications with power conversion efficiencies (PCEs) and mobilities reaching 4.84% and $0.15 \text{ cm}^2 \text{ V}^{-1} \text{ s}^{-1}$, respectively.⁹ It is worth mentioning that a PCE of 2.0% was obtained for a simple TIPS-appended anthanthrene derivative.¹⁰

We recently undertook the derivatization of the commercially available hexacyclic pigment 4,10-dibromoanthanthrene (VAT Orange 3, compound 1 in Scheme 2) and were able to tune its optoelectronic properties through functionalization at the 4 and 10 positions and the 6 and 12 positions on either quinoidal or fully aromatic anthanthrene derivatives.^{11,12} The nature of the linker between the polycyclic core and the appended moiety appeared to be of the utmost importance, mainly because of steric constraints. We were therefore drawn to study the effect of freely rotating acetylenic linkers in order to extend the π -conjugation of anthanthrene and anthanthrene derivatives.

A second point of order was to assess the contribution of the conjugation axis on the resulting properties. Conjugation pathways in polycyclic aromatic molecules are nontrivial, as many parameters, such as the resonance energy, must be taken into account.^{12,13} The two conjugation axes studied are depicted in Figure 1: the lengthwise 4,10 axis is depicted in blue, whereas the 6,12 axis along the width is represented in red. Although 4,10-dibromoanthanthrene presents a versatile structure, its chemical functionalization is not always straightforward, so special attention was paid to the synthetic aspects with respect to practical considerations. Herein we report the synthesis of 4,10-arylethynylantranthrene and

Received: December 3, 2013

Published: February 25, 2014

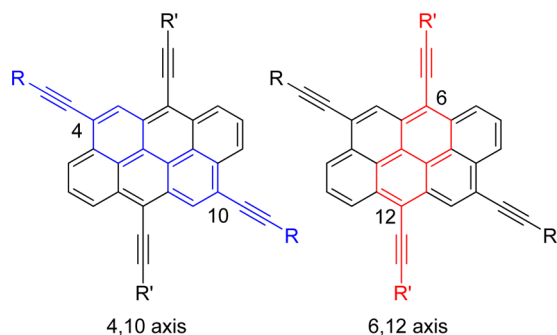


Figure 1. Numbering of anthanthrene positions and depiction of the 4,10 and 6,12 conjugation axes (shown in blue and red, respectively).

4,6,10,12-tetrasubstituted anthanthrene derivatives along with a structure–property relationship analysis of their optoelectronic properties.

RESULTS AND DISCUSSION

Synthesis. The targets are depicted in Figure 2, and the rationale and synthesis is described herein. As first synthetic targets, we chose to study anthanthrones functionalized at the 4 and 10 positions with arylethynyl moieties (as opposed to the previously reported nonconjugated ethynyltriisopropylsilyl moiety¹¹) to assess the effect of the acetylenic linker on the optoelectronic properties of quinoidal anthanthrone and aromatic anthanthrene scaffolds. We previously functionalized 4,10-dibromoanthanthrone through Sonogashira coupling, so we followed this efficient strategy for the introduction of alkynes onto the anthanthrone/anthanthrene scaffold.¹¹ To obtain good solubility and film-forming properties, we chose compounds **2** (Scheme 2)¹⁴ and **4** (Scheme 1) with hexyl and octyl alkyl chains, respectively. Compound **4** was prepared by coupling of 2-bromo-4-octylthiophene and 2-methylbut-3-yn-2-ol using a highly active catalyst derived from $\text{PdCl}_2(\text{MeCN})_2$ and $t\text{Bu}_3\text{PHBF}_4$.¹⁵ Free alkyne **4** was obtained using KOH-promoted deacetonative deprotection in hot toluene. A protecting group bearing a polar alcohol group was chosen to ease the purification by column chromatography.

The introduction of solubility-inducing groups in the first synthetic step was crucial because 4,10-dibromoanthanthrone **1** has very limited solubility, and this was a major criterion when determining the optimal retrosynthetic pathway. The couplings between anthanthrone **1** and terminal alkynes **2** and **4** were performed under classical Sonogashira coupling conditions using *o*-dichlorobenzene (*o*-DCB) as the solvent, which offers a higher reaction rate and improved reproducibility compared with THF (Scheme 2). Phenyl-appended **5** was isolated in 58% yield, but to our surprise, the yield of compound **6** dropped drastically to 12% for unknown reasons. Double nucleophilic attack of the lithium acetylide of compound **2** on the quinone structure followed by reduction with aqueous SnCl_2 afforded anthanthrene **7** in a mere 25% yield. Because of the low solubility of compound **7** in the eluent used in the purification process, the yield was unsatisfactory. Because purity is of utmost importance in organic electronics, we decided to explore alternative synthetic pathways in order to determine the most versatile, straightforward, and efficient strategies.

As depicted in Scheme 3, an obvious alternative was to exchange the order of the two synthetic steps and start with the alkynylation/reduction sequence. To our surprise, we could isolate only traces of phenyl-appended compound **8**. Alternatively, when

the reaction was performed with lithium triisopropylsilylacetylide, the desired compound **9** was isolated in a moderate 48% yield. It was possible to perform the same reaction with trimethylsilylacetylene (TMSA), but the solubility of the resulting product was much lower. The major difference between the two substrates lies in the electronic character of the acetylenic unit. Because of the poor reliability and difficult analysis of side products, we decided not to investigate this reaction further, instead proceeding with TIPS-appended compound **9** because of its versatility and ease of preparation.

From a synthetic perspective and following our objective of studying the effect of the acetylenic linker, we were interested in preparing 4,6,10,12-thienyl-appended compound **11**. Contrary to arylethynyl compounds, 2-thiophenyllithium proved to be a suitable reagent for the preparation of compound **11** (39% yield) from compound **10** (Scheme 4).¹¹ The stronger nucleophilic character of the 2-thiophenyllithium might be responsible for this improved reactivity.

In order to properly establish the effect of the acetylenic linkage on the optoelectronic properties, we prepared compounds **16** and **18** with thiophene units at the 4, 6, 10, and 12 positions but with different linkers (Scheme 5). Starting from compound **9**, we performed a twofold Sonogashira coupling with compound **4** under standard conditions to provide compound **15** in 74% yield. Subsequent deprotection of the alkyne using tetrabutylammonium fluoride (TBAF) afforded the terminal alkyne in excellent yield. Although the TBAF-mediated deprotection of alkynes is a seemingly straightforward step, it proved to be crucial to use water as the proton source for both TMS and TIPS deprotection to obtain the desired products in good yields with minimal formation of side products. The use of methanol as an additive proved to be unsuitable. The following step consisted of a second twofold Sonogashira coupling with 2-bromo-5-octylthiophene. For this particularly demanding coupling reaction of a bisacetylenic compound, it was important to use a $\text{Pd}(0)$ source since the reduction of the $\text{Pd}(\text{II})$ species would consume 2 equiv of alkyne, which would greatly affect the yield in this case as the alkyne was the limiting reagent and could not be used in excess.¹⁶ Therefore, we used a combination of $\text{Pd}_2(\text{dba})_3$ and $t\text{Bu}_3\text{PHBF}_4$ as a precatalyst for the coupling of electron-rich bromoarenes. Using these optimal conditions, we obtained compound **16** in an excellent 80% yield. Compound **18** with thiophenes directly attached at the 4 and 10 positions was prepared using the same strategy, but the first reaction step consisted of a Stille coupling using an in situ-prepared stannyl compound. Compound **17** proved to be insoluble in THF, so the deprotection reaction was performed in CH_2Cl_2 , followed by the twofold Sonogashira coupling with the bromothiophene to afford compound **18** in excellent yield.

In order to assess the presence of intramolecular charge transfer through donor–acceptor interactions, we prepared electron-donating thiothiophene derivative **13** and electron-withdrawing sulfonylthiophene derivative **14**. The sulfonylthienyl group has been used in high-performance polymers for solar cells^{17,18} and was chosen because the electroactive group is located linearly with the conjugation axis, thus leading to a greater impact on the properties. As depicted in Scheme 6, thiophene was lithiated using *n*-BuLi and added to elemental sulfur to form the thiolate, which was alkylated using 2-ethylhexylbromide to afford compound **12** in good yield. Subsequent bromination using NBS afforded compound **13** almost quantitatively, and the thioether was oxidized with *m*-CPBA to give sulfone **14**.

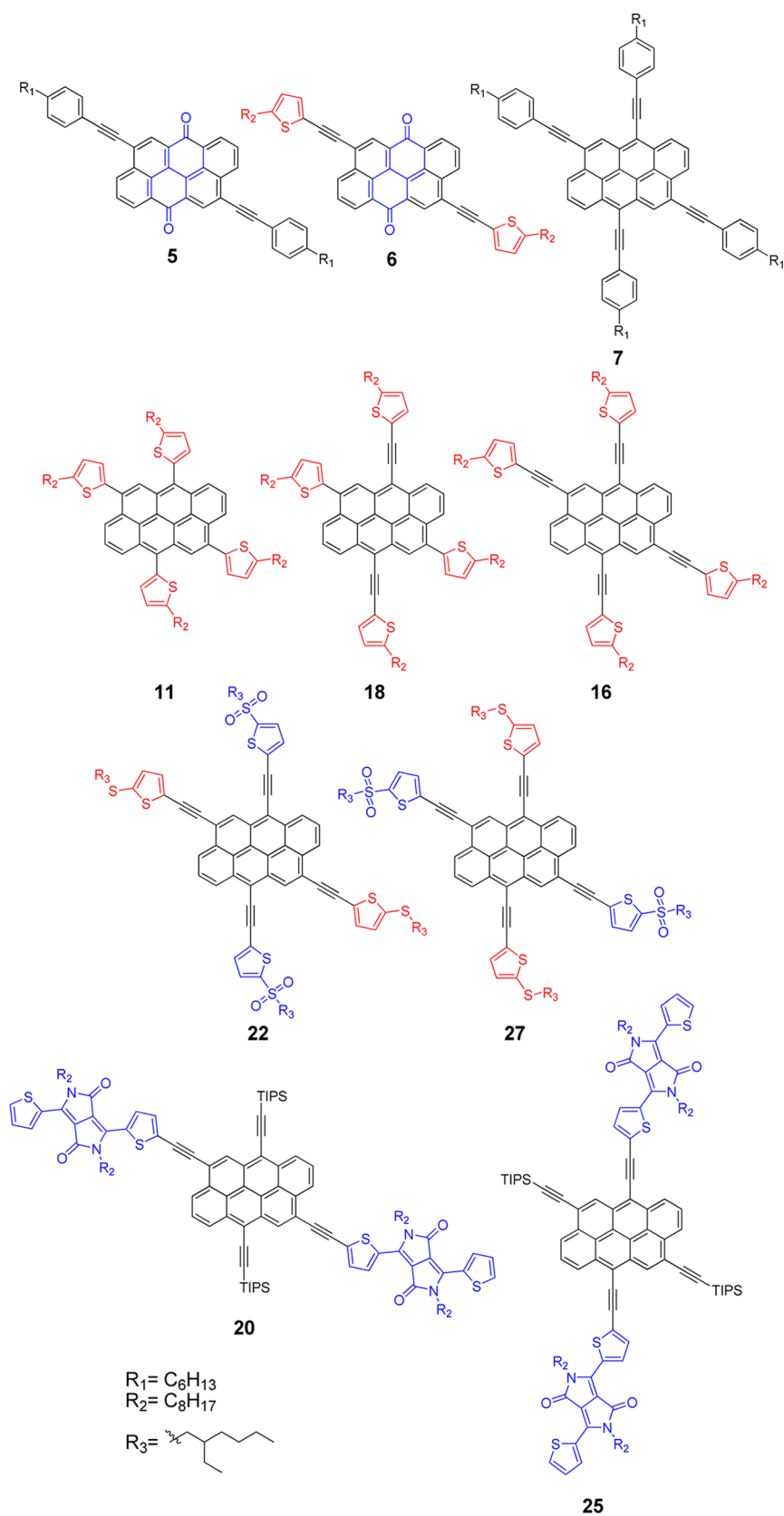
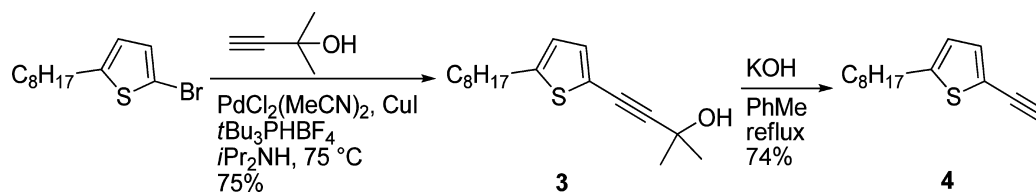


Figure 2. Structures of π -extended compounds **5**, **6**, **7**, **11**, **16**, **18**, **20**, **22**, **25**, and **27**. Donor and acceptor groups are depicted in red and blue, respectively.

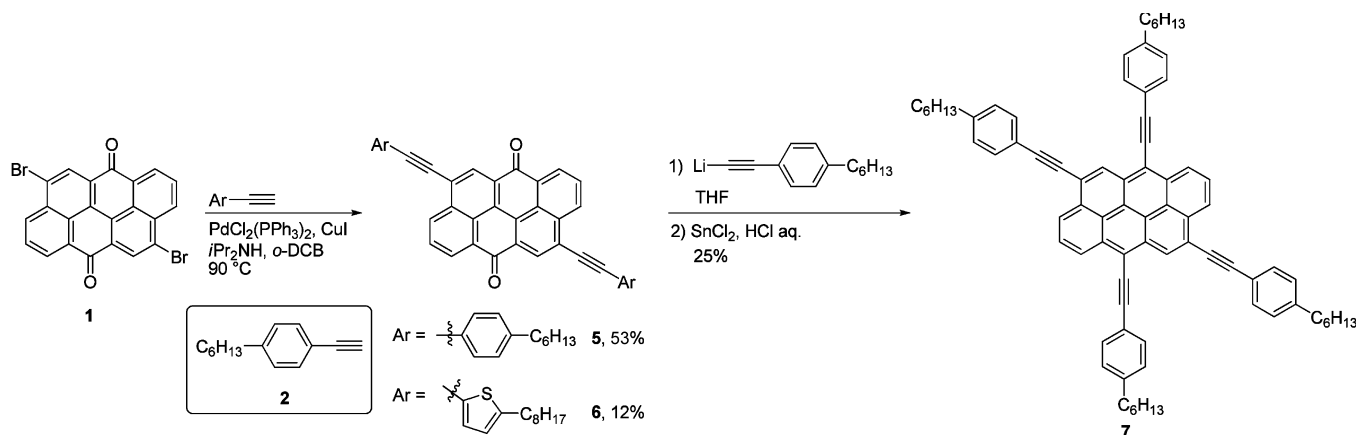
Once again starting with TIPS-appended compound **9**, we introduced TMS-acetylene at the 4 and 10 positions via standard Sonogashira coupling to afford compound **19** in excellent

yield (Scheme 7). Selective deprotection of the TMS-acetylene using K_2CO_3 followed by twofold Sonogashira coupling with a monobromo-substituted diketopyrrolopyrrole (DPP) reagent¹⁹

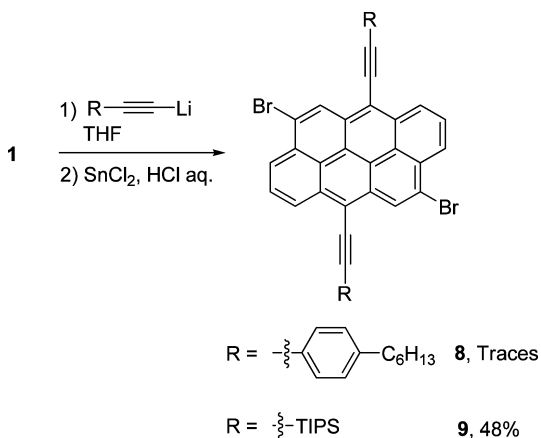
Scheme 1. Synthesis of 2-Ethynyl-5-octylthiophene (4)



Scheme 2. Synthesis of Anthanthrones 5 and 6 and Anthanthrene 7



Scheme 3. Synthesis of 6,12-Ethynyl-Appended 4,10-Dibromoanthanthrones 8 and 9



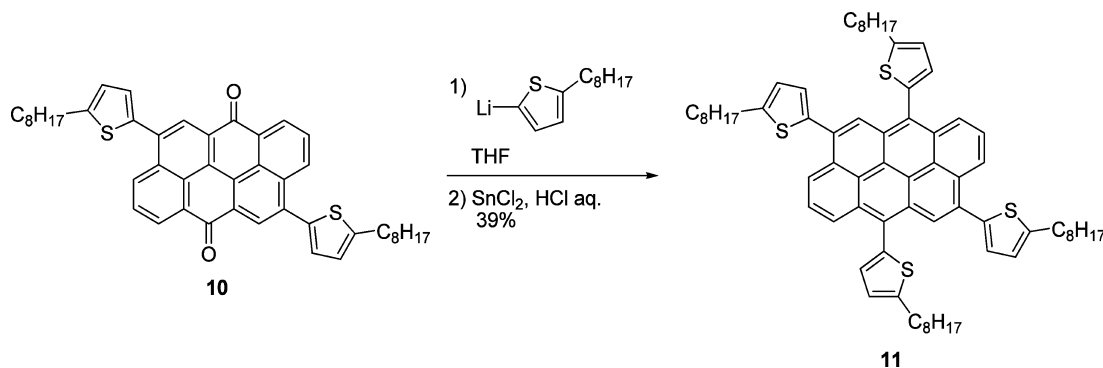
afforded the π -extended compound **20** in 49% yield. Alternatively, electron-rich compound **13** was coupled using the same conditions to afford compound **21**. Following the previously described

strategy, we obtained the 4,10-donor-6,12-acceptor-appended compound **22** from compounds **21** and **14** in excellent yield.

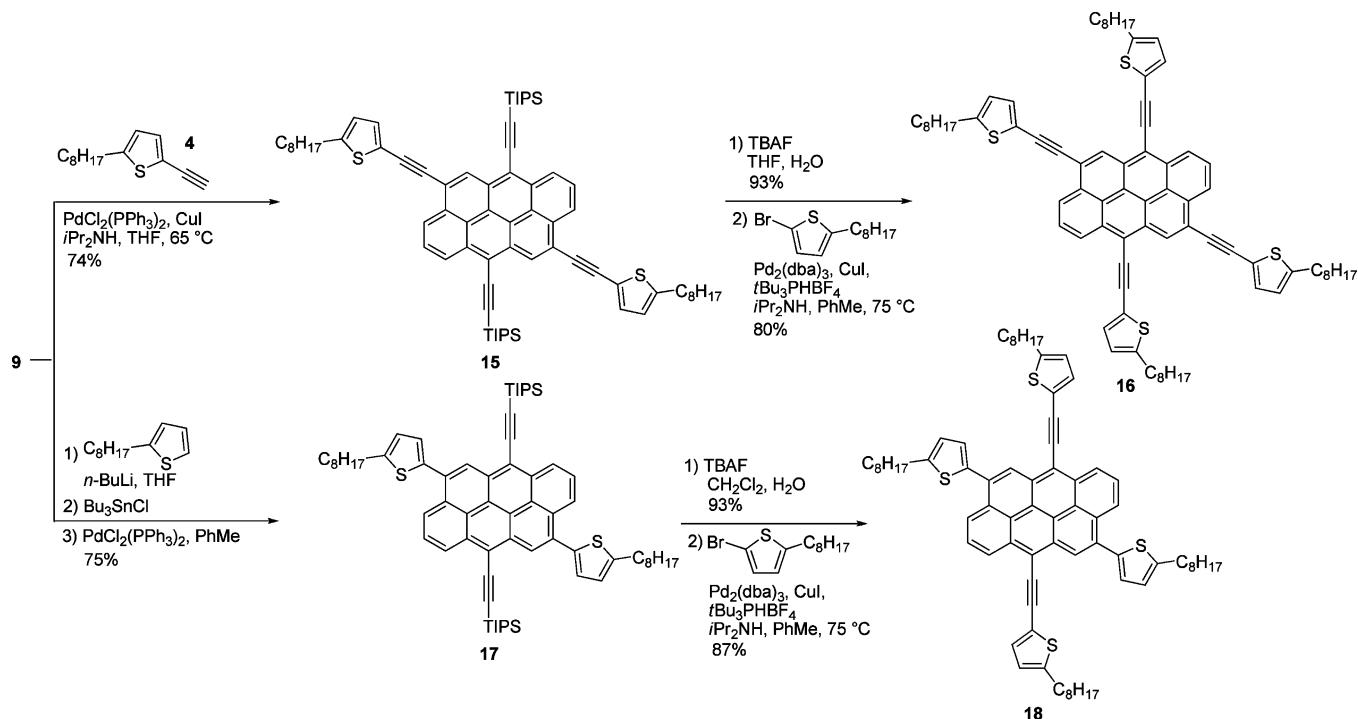
To obtain the opposite substitution pattern (4,10-acceptor-6,12-donor) for the sake of comparison, we chose to start from soluble TIPS-appended **23**¹¹ and to introduce TMS-acetylene substituents at the 6 and 12 positions via a one-pot twofold carbonyl attack/reduction sequence (Scheme 8). Aryl groups were then introduced at the 6 and 12 positions via selective deprotection of the TMS-acetylene followed by a coupling step with the corresponding aryl bromides to afford DPP-appended compound **25** and thiothiophene-substituted compound **26** in 62% and 94% yield, respectively. Compound **27** was obtained from **26** and **14** in a lower 31% yield for the last coupling step, the reasons for which are unclear.

Optical Properties. The UV-vis spectra of the anthanthrone and anthanthrene compounds were recorded in CH_2Cl_2 solutions at concentrations of 10–50 μM or in thin films prepared by drop-casting from CH_2Cl_2 on glass slides, and these spectra are presented in Figures 3–7 or in the Supporting Information. The fluorescence spectra were recorded in CH_2Cl_2 and are presented in the Supporting Information. The optical properties are summarized in Table 1.

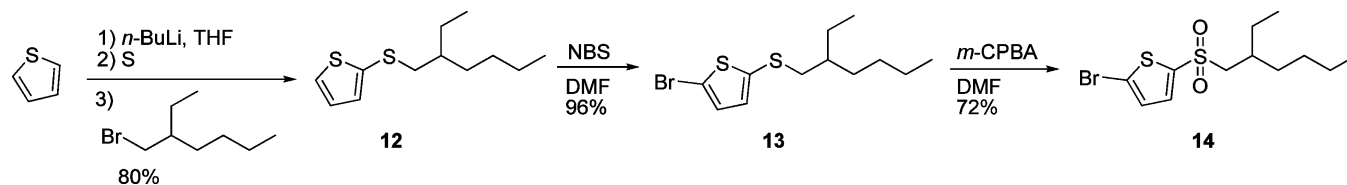
Scheme 4. Synthesis of 4,6,10,12-Tetrakis((5-octyl)thien-2-yl)anthanthrene (11)



Scheme 5. Synthesis of Tetrakis(thienyl)anthanthrene Derivatives 16 and 18 with Different Acetylenic Linkages



Scheme 6. Synthesis of Thiothienyl Compound 13 and Sulfonylthienyl Compound 14



Both of the 4,10-bis(arylethynyl)anthanthrene derivatives present broad absorption spectra with $\lambda_{\max} = 545$ and 570 nm for compounds **5** and **6**, respectively (Figure 3), in accordance with the stronger donating character of the thiophene unit, which leads to a stronger donor–acceptor interaction with the accepting quinone. This interaction is especially marked in the solid state, as the band gap for compound **6** is lowered by 0.32 to 1.66 eV. To measure the effect of the acetylenic linkage, we can compare compound **6** with previously reported compound **10** (Scheme 4):¹¹ the absorption maximum of compound **6** is red-shifted by 35 nm, which is indicative of good electronic communication between the two appended units, reasonably caused by the reduced torsion angle of the acetylenic linkage.

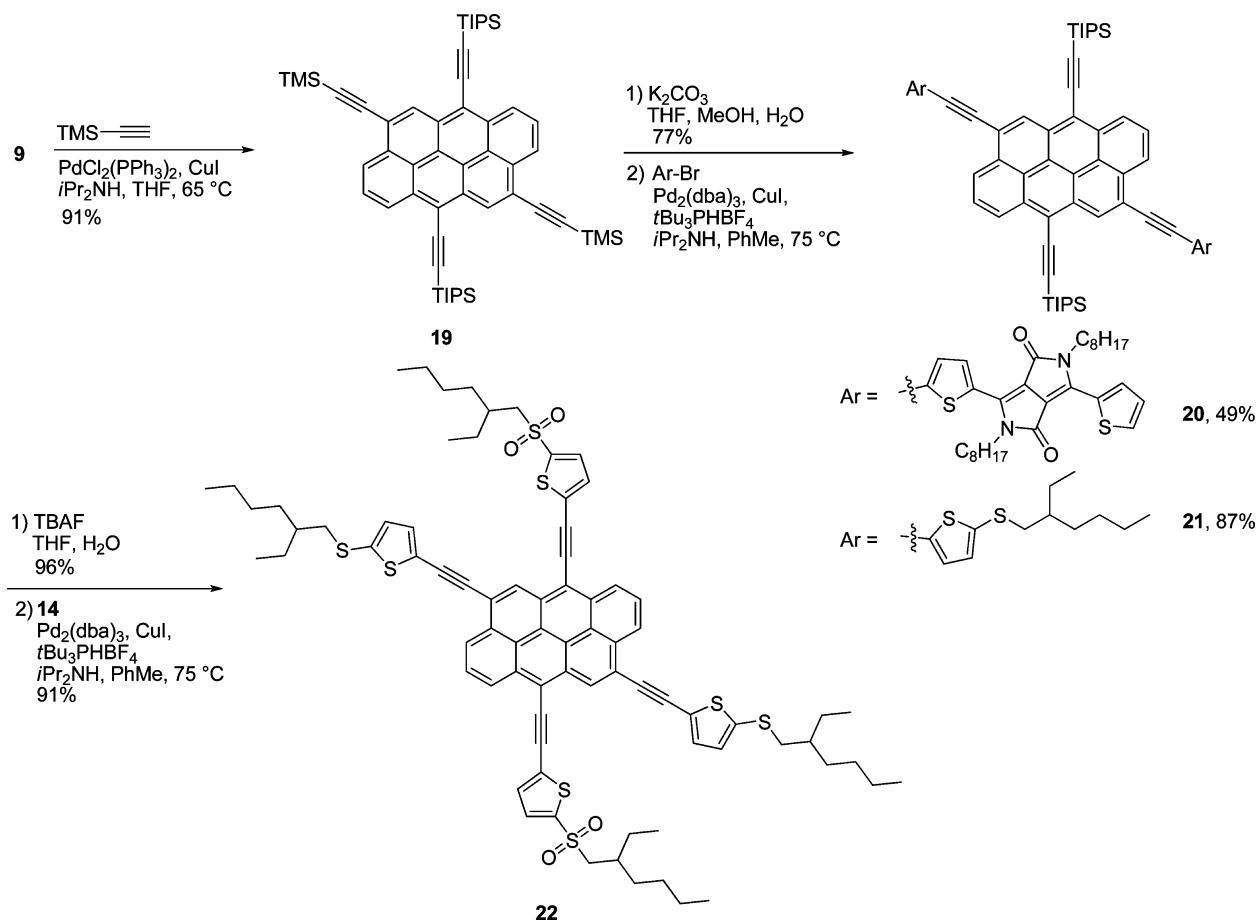
For the thienyl- and phenyl-appended anthanthrene compounds, it is clear that the acetylenic linkage at the 6 and 12 positions is necessary for effective conjugation. Ethynyl-free compound **11** presents the shortest λ_{\max} of 465 nm, whereas introduction of the acetylene linker in compound **18** causes a large red shift of 68 nm to a maximum of 533 nm (Figure 4). The relief of the large dihedral angle (calculated value of 90°) caused by the steric hindrance between the *peri* positions and the thiophene ring is the major contributor to the improved conjugation. Incorporation of acetylenic linkers at the 4 and 10 positions for compound **16** has a much weaker effect on the absorption, with a slight red shift of 7 nm. Interestingly, phenyl-appended compound **7** presents a moderately blue-shifted λ_{\max}

of 519 nm, which can be attributed to the weaker donating character of the phenyl unit versus the thienyl unit.

As presented in Figure 5, the thin-film absorption spectra of compounds **7** and **16** are very similar, with the exception of a slightly broader peak for compound **7**, meaning that in this case the nature of the appended aromatic unit has a limited effect on the solid-state absorption profile. Nevertheless, the solid-state band gap is lowered by 0.39 eV down to 1.91 eV for compound **7**. Such a large modulation is indicative of good intermolecular interaction and orbital overlap, which supports the NMR aggregation study (vide infra). It is reasonable to think that for compound **11** the steric hindrance limits close intermolecular interactions, leading to a large band gap of 2.35 eV. On the other hand, compound **18** presents the smallest band gap of 1.90 eV, indicating that the presence of thiophene units at the 4 and 10 positions does not limit close intermolecular interactions. Compound **18** presents the most characteristic features of J-aggregation, with a large bathochromic shift in going from dilute solution to the solid state, the narrowest absorption band, and most intense absorption at its maxima.²⁰ This suggests that the increased latitude along the 4,10 axis for the acetylenic-substituted derivatives **11** and **16** might hinder optimal J-aggregation.

The absorption spectra of compounds **22**, **26**, and **27** with λ_{\max} values of ca. 545 nm (Figure 6) are very similar to that of compound **16**, revealing a lack of intramolecular donor–acceptor interactions. Moreover, substitution of the electronically neutral TIPS group in compound **26** by sulfonylthiophene

Scheme 7. Synthesis of 4,10-DPP-Appended Anthanthrene 20 and Donor–Acceptor-Substituted Compound 22



Scheme 8. Synthesis of 6,12-DPP-Appended Anthanthrene 25 and Donor–Acceptor-Substituted Compound 27

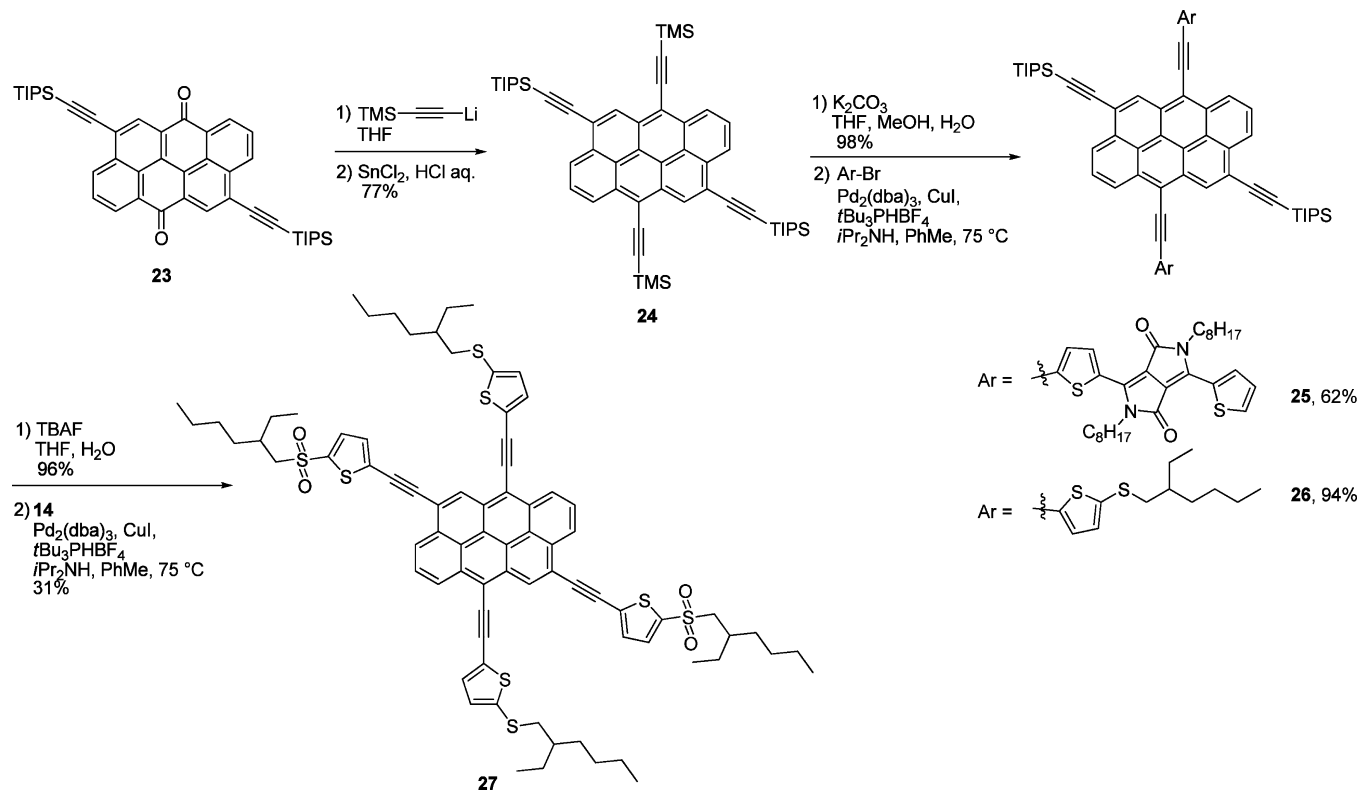
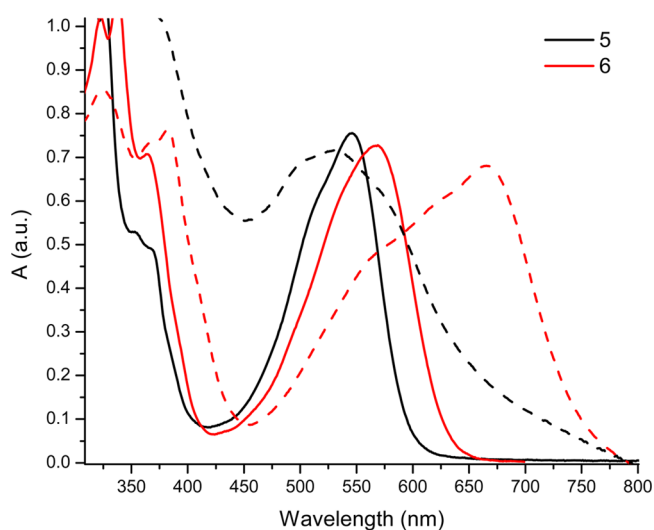


Table 1. Summary of the Optical and Electrochemical Properties of Selected Compounds^a

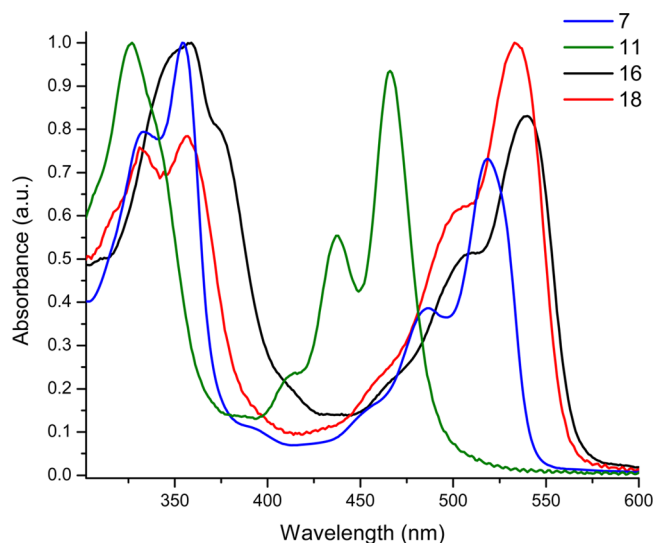
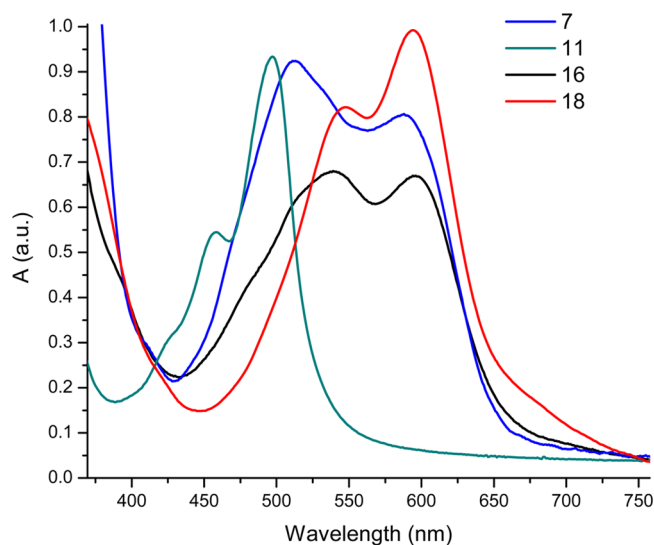
compd	optical properties				electrochemical properties		
	λ_{\max} (nm)	$E_{\text{g}}^{\text{soln}}$ (eV)	λ_{fluor} (nm)	$E_{\text{g}}^{\text{film}}$ (eV)	V_{red} (V)	V_{ox} (V)	E_{g} (eV)
5	545	2.08	608	1.83	−0.50	1.47	1.97
6	570	1.98	654	1.66	−0.51	1.30	1.81
7	519	2.30	538	1.91	−1.10	0.70	1.80
9	491	2.46	528	2.12	−1.06	1.08	2.14
11	465	2.53	495	2.35	−1.40	0.77	2.17
15	505	2.37	513	2.18	−1.07	0.94	2.01
16	540	2.19	560	1.91	−1.05	0.66	1.71
17	501	2.38	516	2.20	−1.21	0.85	2.06
18	533	2.23	552	1.90	−1.13	0.58	1.71
19	499	2.42	507	2.34	−1.09	0.97	2.06
20	588	1.97	627	1.71	−1.01	0.74	1.75
21	505	2.37	521	2.17	−1.09	0.89	1.98
22	538	2.20	557	1.88	−0.93	0.91	1.84
24	498	2.44	505	2.30	−1.10	0.97	2.07
25	650	1.76	—	1.46	−0.90	0.75	1.65
26	545	2.15	578	1.79	−1.05	0.65	1.70
27	547	2.13	595	1.86	−0.99	0.78	1.77

^a $E_{\text{g}}^{\text{soln}}$ and $E_{\text{g}}^{\text{film}}$ were measured at the onset. V_{red} and V_{ox} were measured at the current onset in V vs Ag/AgCl at a scan rate of 100 mV s^{−1}. $E_{1/2}$ for Fc/Fc⁺ was measured at 0.45 V vs Ag/AgCl.

**Figure 3.** UV-vis absorption spectra of compounds **5** and **6** in CH₂Cl₂ solution (solid lines) and thin films (dashed lines).

units in compound **27** has a negligible effect on the absorption spectra, analogous to cross-conjugated systems.²¹ The poorly defined thin-film absorption profiles of the three molecules could be indicative of weak intermolecular interactions even in the solid state. Interestingly, thiothienyl-appended compound **26** has the smallest band gap at 1.79 eV, which could indicate that the bulkier sulfonyl group hinders close intermolecular interactions.

Comparison of DPP-appended compounds **20** and **25** allows for the unambiguous determination of whether the 4,10 axis or the 6,12 axis is the most effective conjugation axis. In the solution absorption spectrum of 4,10-DPP-appended compound **20** (Figure 7), there is a sharp peak at 507 nm that can be assigned to the absorption profile of the tetrakis(ethynyl)-anthanthrene (see Figure S8 in the Supporting Information),

**Figure 4.** Solution UV-vis absorption spectra of compounds **7**, **11**, **16**, and **18**.**Figure 5.** Thin-film UV-vis absorption spectra of compounds **7**, **11**, **16**, and **18**.

meaning that the conjugation between the two units is quite limited. The introduction of DPP units at the 6 and 12 positions in compound **25** causes a red shift of λ_{\max} by 62 nm (vs compound **20**) to 650 nm, indicating more effective conjugation. A small band gap of 1.46 eV was obtained for thin films of compound **25**, indicating good intermolecular interactions in the solid state.

Photostability. All of the synthesized anthanthrene compounds proved to be highly stable under standard laboratory conditions, which is a significant advantage over linearly fused acenes such as anthracene and pentacene derivatives that suffer from photooxidation.²² To assess the stability of the anthanthrene scaffold, compound **16** was studied as a representative example. A 10 μ M solution of **16** in CH₂Cl₂ was irradiated in a glass vial in air for 60 min under a 500 W halogen lamp and compared against a sample kept in the dark. Illumination under the high-power white light had a negligible effect on the absorption profile (Figure 8). We attribute this improved photostability to the absence of a reactive diene and

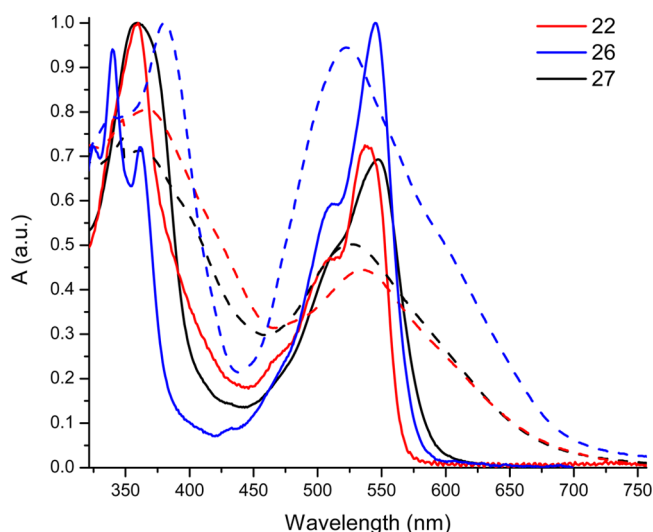


Figure 6. Solution (solid lines) and thin-film (dashed lines) UV-vis absorption spectra of compounds 22, 26, and 27.

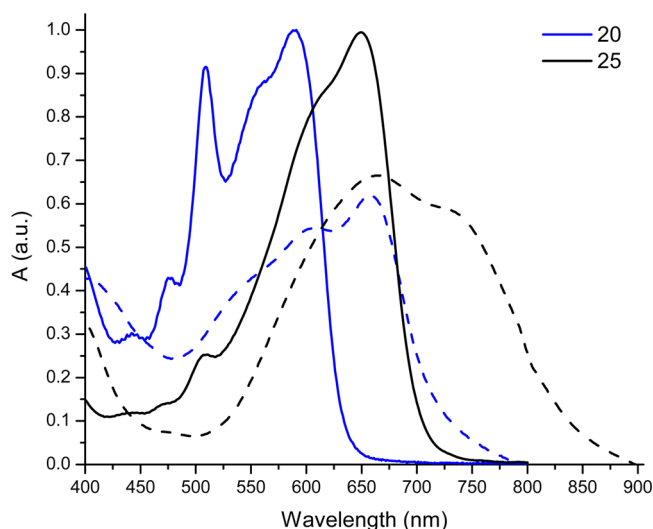


Figure 7. Solution (solid lines) and thin-film (dashed lines) UV-vis absorption spectra of DPP-appended compounds 20 and 25.

the more rigid structure of the fused polycyclic core as opposed to linearly fused acene.²²

Solution Aggregation Study. The absorption red shift of compound 7 prompted us to study its solution aggregation behavior, and we chose to perform this study via ¹H NMR spectroscopy in CHCl₃ at different concentrations. The NMR spectra of the aromatic region at concentrations ranging from 0.8 to 35 mg/mL are presented in Figure 9. The singlet resonance labeled with a red dot is assigned to the anthanthrene protons at the 5 and 11 positions and is strongly shifted upfield by up to 0.57 ppm with increasing concentration. The resonances for the other anthanthrene aromatic protons (peaks just above 8.2 ppm for the 0.8 mg/mL spectrum) are also shifted to a similar extent, whereas the chemical shifts of the signals associated with the phenyl groups are less influenced. Upfield shifts are generally indicative of face-to-face interactions in aromatic systems.²³ Using a monomer-dimer model,^{24,25} we were able to determine an association constant of 84 M⁻¹ (Figure S12 in the Supporting Information). Although a direct comparison of the association constants with those of the parent structures is difficult, this value lies between the

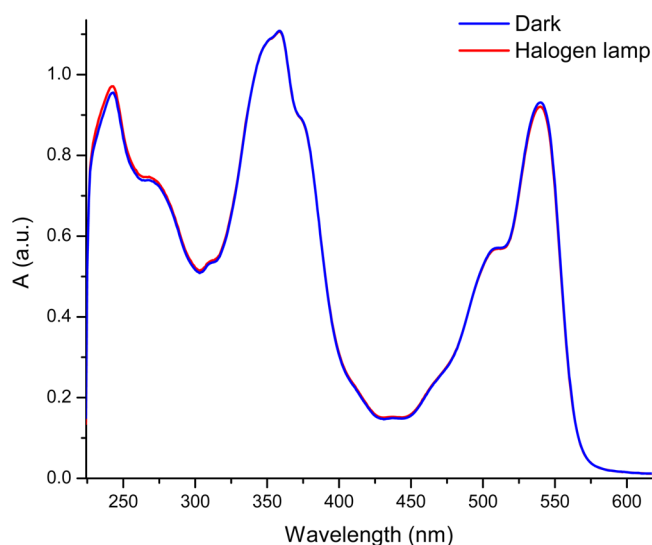


Figure 8. Photostability of compound 16 under illumination with white light from a halogen lamp.

values determined for a polycyclic hexabenzocoronene (HBC-C12) ($K_a = 484 \text{ M}^{-1}$)²⁶ and phenylacetylene macrocycles (PAMs) ($K_a = 39 \text{ M}^{-1}$),²⁵ which suggests that the intermolecular interactions are surprisingly strong for a carbon-rich, heteroatom-free molecule. It is reasonable to think that such interactions could lead to liquid-crystalline properties in the solid state with appropriate side chains, although studies in this direction have not yet been undertaken.

Electrochemistry. In order to determine the redox potentials and the positions of the frontier orbitals, we performed cyclic voltammetry in CH₂Cl₂ with Bu₄NPF₆ as the electrolyte, a Ag/AgCl reference electrode, and a platinum wire working electrode. The potentials were measured at the current onset and are reported in Table 1.

As presented in Figure 10, both of the anthanthrene derivatives 5 and 6 present two reversible and well-defined reduction peaks typical of anthanthrene compounds¹¹ with very similar potentials of −0.50 and −0.87 V. The major difference between the two compounds lies in the lower oxidation potential of compound 6: substitution of the phenyl group by the electron-rich thiophene moiety lowers V_{ox} by 0.17 V down to 1.30 eV, which is indicative of good electronic communication between the two moieties and corroborates the optical data.

Among the anthanthrene compounds presented in Figure 11, ethynyl-free compound 11 presents the highest oxidation and reduction potentials (0.77 and −1.40 V, respectively). Introduction of the ethynyl linker at the 6 and 12 positions in compound 18 drastically lowers both V_{red} by 0.26 V to −1.13 V and V_{ox} by 0.19 V to 0.58 V. This proves that acetylenic linker is effective at extending the conjugation along the 6,12 axis and stabilizing both the negative and positive charges with highly reversible redox processes. Introduction of the acetylenic linker at the 4 and 10 positions shifts the HOMO–LUMO frontier orbitals down by 0.08 eV for compound 16. Substitution of the thiophene units by phenyl ones in compound 7 increases both V_{red} and V_{ox} by ca. 0.05 V compared with compound 16, corroborating the higher optical band gap.

Analysis of the cyclic voltammograms of compounds 22, 26, and 27 presented in Figure 12 allows the effects of donor and acceptor groups on the redox potentials to be ascertained. 6,12-Sulfonylthiophene-appended compound 22 presents the lowest

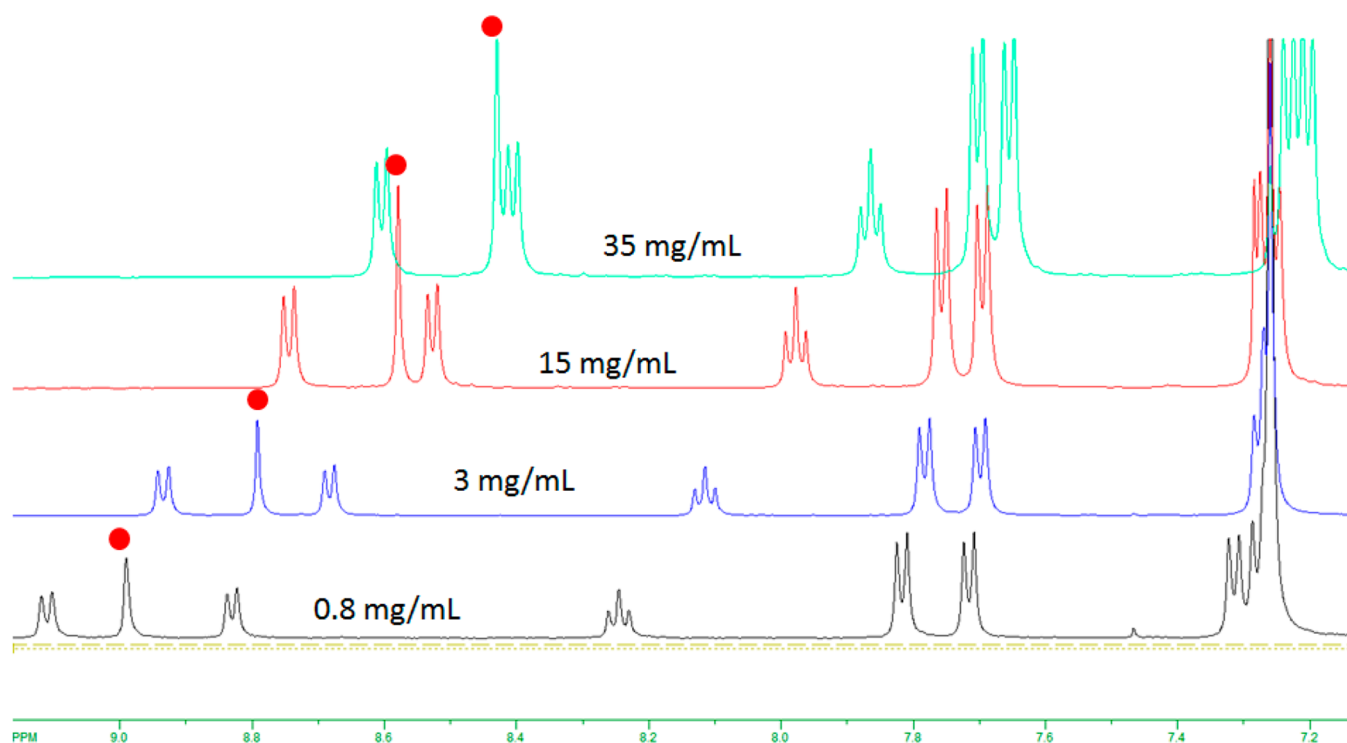


Figure 9. ^1H NMR spectra of ethynylphenyl-appended compound **7** at different concentrations in CDCl_3 at 23°C .

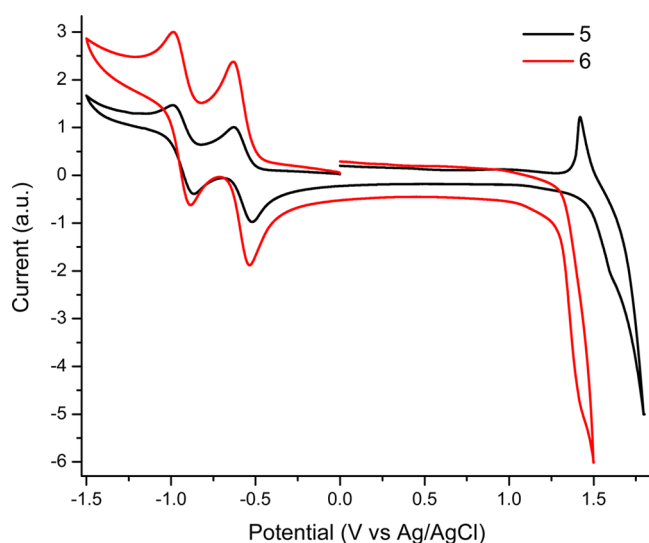


Figure 10. Cyclic voltammograms of anthanthrone compounds **5** and **6**.

reduction potential at -0.93 V , whereas compound **27** has a higher reduction potential at -0.99 V , indicating that the electron-withdrawing group is more effective at stabilizing a negative charge when installed at the 6 and 12 positions. The same trend is observed when the oxidation potentials are compared: 6,12-thiothienyl-appended compound **27** is oxidized at a much lower potential than compound **22** (0.78 vs 0.91 V , respectively). Surprisingly, substitution of the TIPS groups in compound **26** with the sulfonylthiophene in compound **27** increases V_{ox} by 0.13 V , whereas V_{red} is lowered by only -0.06 V and appears to be less reversible.

The two DPP-appended compounds **20** and **25** (Figure 13) present multiple oxidation processes, and the reasons for this

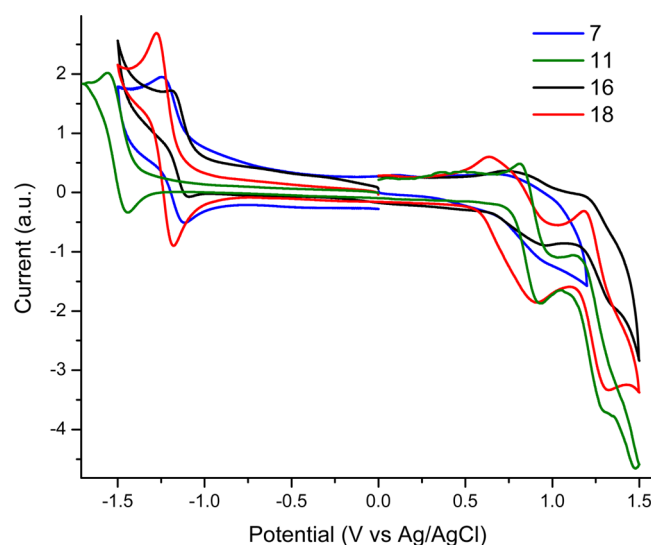


Figure 11. Cyclic voltammograms of anthanthrenes **7**, **11**, **16**, and **18**.

behavior are not well understood at this time. The electrochemical band gap of compound **25** is 1.65 V , which is lowered by 0.10 V compared with that of compound **20**, indicative of the better conjugation along the 6,12 axis. This result corroborates the lower optical band gap observed for the extended conjugation along the 6,12 axis.

To obtain the vacuum levels from the cyclic voltammetry data, the potentials were corrected against an external ferrocene standard measured at 0.45 V vs Ag/AgCl and fixed at 5.1 eV against vacuum. The results are reported in Figure 14.²⁷

DFT Calculations. We performed calculations of the frontier orbitals using the commonly used B3LYP/6-31G* level of theory²⁸ for representative compounds **6**, **11**, **16**, and **18**. The optimized structure of anthanthrone **6** is highly planar

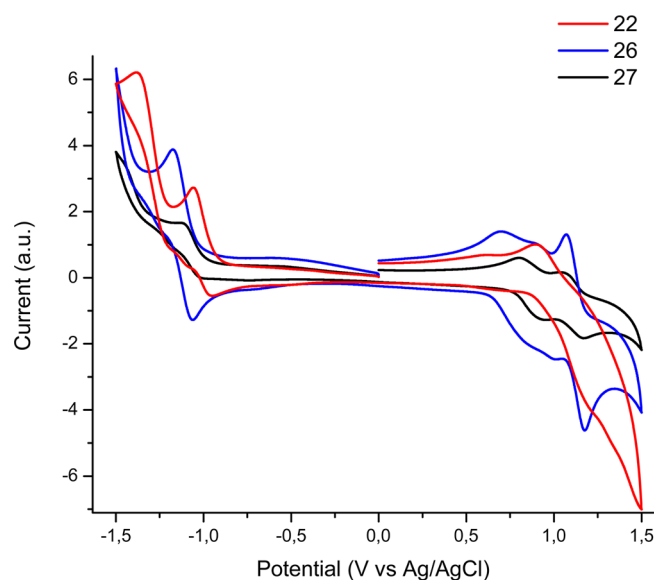


Figure 12. Cyclic voltammograms of compounds 22, 26, and 27.

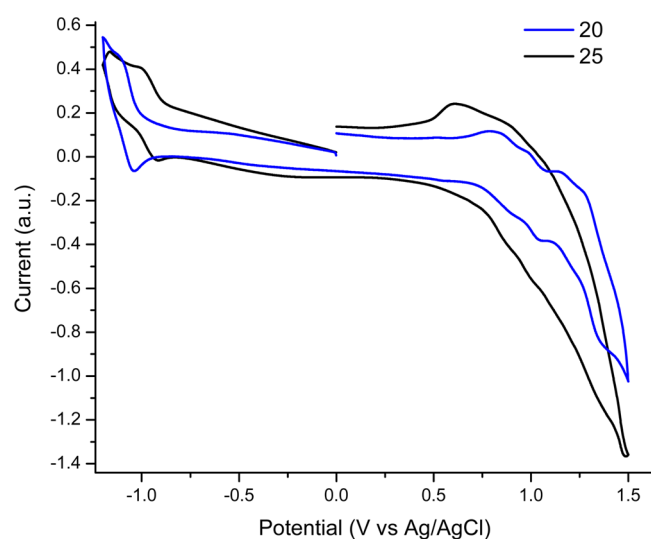


Figure 13. Cyclic voltammograms of DPP-appended compounds 20 and 25.

with a HOMO that is homogeneously distributed lengthwise over the whole molecule along the 4,10 axis, whereas the

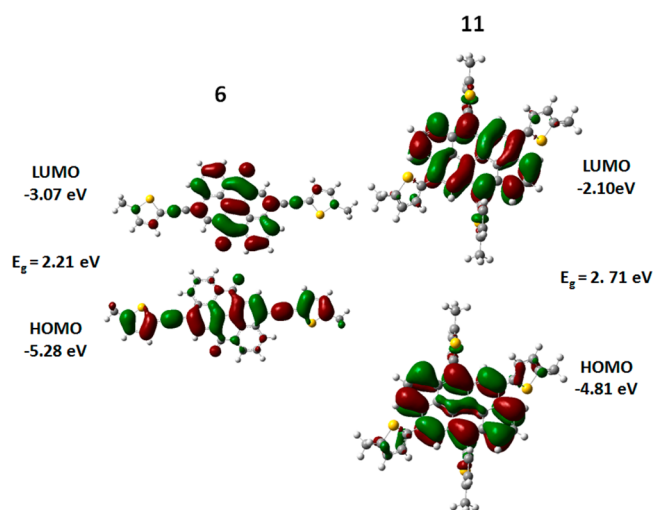


Figure 15. Calculated frontier orbitals for compounds 6 and 11.

LUMO is concentrated on the anthanthrene core along the quinoidal axis as expected (Figure 15). The HOMO and LUMO of compound 11 are mostly localized over the anthanthrene moiety, and the large dihedral angle of 90° between the aromatic planes and the thiophenes at the 6 and 12 positions limit all delocalization beyond the anthanthrene. At the 4 and 10 positions, the smaller but significant calculated dihedral angle of 53° allows limited delocalization over the thiophene.

The distributions of the HOMO and LUMO in compounds 16 and 18 are mostly delocalized over the 6,12 axis (Figure 16), supporting the experiments showing improved conjugation along that axis. The frontier orbitals are hardly delocalized beyond the acetylenic bond at the 4 and 10 positions, once again supporting the negligible effect of appending electroactive units at these positions.

CONCLUSION

Acetylic linkers were successfully used to tune the optoelectronic properties of anthanthrone and anthanthrene derivatives. From a synthetic standpoint, Sonogashira coupling proved to be a highly versatile and efficient tool to attach different electroactive aromatic units, whereas direct nucleophilic attack of lithiated reagents followed by reduction proved to be highly susceptible to electronic effects on both the reagents and reactants. The simple thiophene-appended anthanthrone

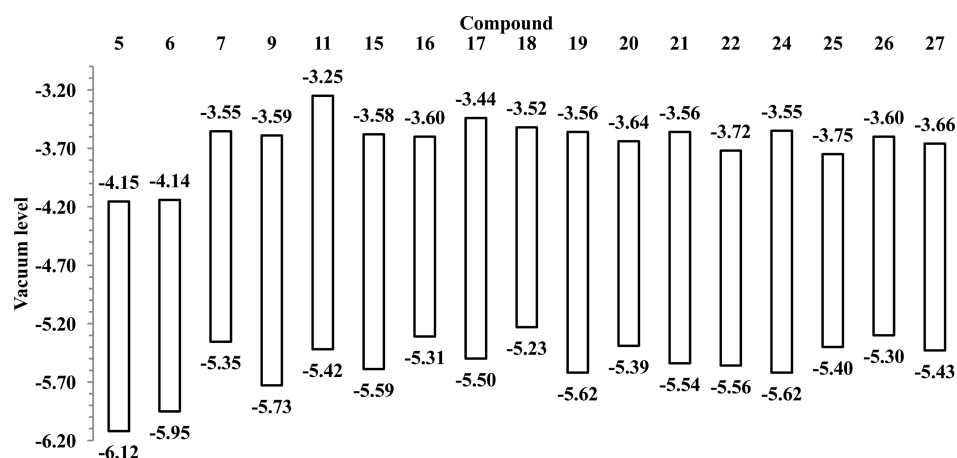


Figure 14. Electrochemically determined (bottom) HOMO and (top) LUMO energy levels for selected compounds.

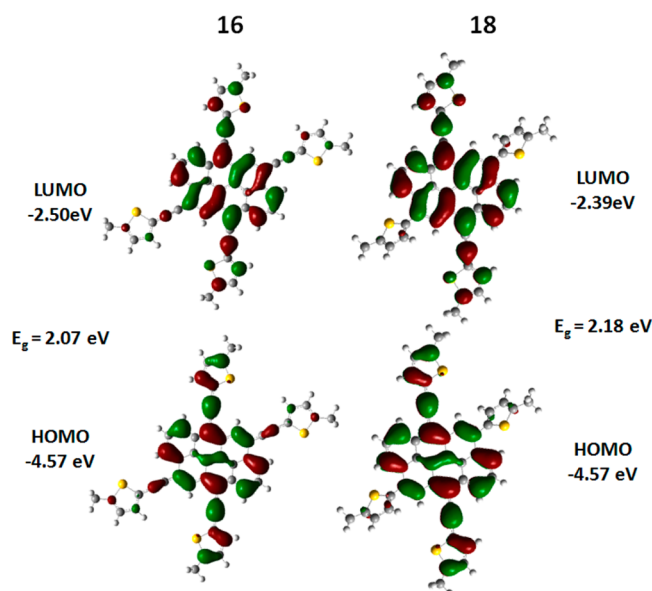


Figure 16. Calculated frontier orbitals for compounds 16 and 18.

derivative 6 with a low band gap of 1.66 eV and a high electron affinity with a LUMO energy of -4.14 eV was prepared and presented potentially attractive properties as an acceptor in solar cells. We determined that the optoelectronic properties of anthanthrene compounds are governed by substitution at the 6 and 12 positions rather than the 4 and 10 positions and that the acetylic linker was essential to relieve the steric strain between the anthanthrene and the appended aromatic unit. Functionalization with different aromatic units allowed precise control of the HOMO and LUMO energy levels. Highly reversible redox processes were generally observed, and low-band-gap materials could be obtained with the proper conjugated units. We assume that the 4 and 10 positions of the anthanthrene unit could be used as a simple way to fine-tune the solubility and packing behavior via side-chain engineering. Strong face-to-face interactions were observed in solution, leading to large red shifts in the solid state indicative of J-aggregation. Such intermolecular interactions should lead to good charge transport properties because of the large intermolecular orbital overlap.⁶ The ease of preparation from commercial products, tailorable properties, excellent photostability, and reversible redox processes of anthanthrene compounds make them excellent candidates for low-cost organic electronic applications. The evaluation of the most promising candidates in OFETs and OPV applications is currently underway along with the preparation of polymeric analogues.

EXPERIMENTAL SECTION

General Methods. 4,10-Dibromoanthanthrone was provided as a courtesy by Heubach GmbH as product Monolite Red 316801. High-resolution mass spectrometry (HRMS) was performed using a time-of-flight (TOF) LC–MS apparatus equipped with an APPI ion source.

Electrochemical Measurements. All of the cyclic voltammograms were acquired employing a three-electrode potentiostat. The potential was referenced to a Ag/AgCl-saturated KCl electrode, and Pt wires were used as the working and counter electrodes. CH_2Cl_2 with a supporting electrolyte of Bu_4NPF_6 (0.1 M) was sparged using argon 5 min prior to electrochemical measurements. For calculation of vacuum levels, the potentials were calibrated against a ferrocene/ferrocenium external standard measured at 0.45 V versus the Ag/AgCl reference electrode.

Computational Methods. DFT calculations were carried out with the Gaussian 09 program suite²⁸ at the B3LYP/6-31G* level of theory, and the orbital plots are reported at an isovalue of 0.02.

2-Methyl-4-(5-octylthiophen-2-yl)but-3-yn-2-ol (3). A dry flask under nitrogen was charged with 2-bromo-5-octylthiophene (1.5 g, 5.72 mmol), dichlorobis(acetonitrile)palladium(II) (14 mg, 0.057 mmol), tri-*tert*-butylphosphonium tetrafluoroborate (33 mg, 0.114 mmol), and copper(I) iodide (11 mg, 0.057 mmol), and the flask was flushed three times with a vacuum/nitrogen cycle. Diisopropylamine (5.7 mL) was deaerated using a continuous flow of nitrogen for 10 min and transferred via syringe to the reaction flask. The reaction mixture was heated to 70 °C, and 2-methylbut-3-yn-2-ol (721 mg, 8.58 mmol) was added dropwise. A white precipitate was quickly formed, and the reaction mixture was heated for 1 h at this temperature. Once the mixture cooled, a saturated NH_4Cl solution was added, and the aqueous layer was extracted three times with CH_2Cl_2 . The organic layer was dried with MgSO_4 , and the solvent was evaporated under reduced pressure. The crude product was purified by silica gel column chromatography (AcOEt/hexanes 5:95 to 10:90 v/v) to afford compound 3 as a colorless oil (1.20 g, 75%). ^1H NMR (400 MHz, CDCl_3): δ 6.99 (d, J = 3.7 Hz, 1H), 6.62 (d, J = 3.4 Hz, 1H), 2.76 (t, J = 7.3 Hz, 2H), 2.05 (s, 1H), 1.68–1.58 (m, 9H), 1.37–1.22 (m, 10H), 0.88 (t, J = 7.0 Hz, 3H). ^{13}C NMR (100 MHz, CDCl_3): δ 148.1, 132.0, 123.9, 119.8, 96.6, 76.0, 65.7, 31.8, 31.5, 31.3, 30.1, 29.3, 29.2, 29.0, 22.7, 14.1. HRMS (APPI+): calcd for $\text{C}_{17}\text{H}_{27}\text{OS}$ ($M + \text{H}$)⁺ 279.1777, found 279.1782.

2-Ethynyl-5-octylthiophene (4). A dry flask equipped with a reflux condenser under nitrogen was charged with 2-methyl-4-(5-octylthiophen-2-yl)but-3-yn-2-ol (3) (1.2 g, 4.3 mmol), potassium hydroxide (724 mg, 12.9 mmol), and anhydrous toluene (65 mL), and the resulting solution was deaerated with a continuous flow of nitrogen for 5 min and then heated to a vigorous reflux for 30 min. Once the mixture was cooled to room temperature, hexanes (65 mL) was added, and the crude mixture was poured onto a silica gel pad and eluted with hexanes to afford compound 4 as a colorless oil (702 mg, 74%). ^1H NMR (400 MHz, CDCl_3): δ 7.09 (d, J = 3.5 Hz, 1H), 6.63 (d, J = 3.1 Hz, 1H), 3.29 (s, 1H), 2.77 (t, J = 7.4 Hz, 2H), 1.69–1.60 (m 2H), 1.39–1.19 (m, 10H), 0.88 (t, J = 5.8 Hz, 3H). ^{13}C NMR (100 MHz, CDCl_3): δ 148.6, 133.1, 123.9, 119.2, 80.4, 77.5, 31.9, 31.6, 30.1, 29.3, 29.2, 29.0, 22.7, 14.1. HRMS (APPI+): calcd for $\text{C}_{14}\text{H}_{21}\text{S}$ ($M + \text{H}$)⁺ 221.1358, found 221.1370.

4,10-Bis((4-hexylphenyl)ethynyl)anthanthrone (5). A dry flask under nitrogen was charged with 1-ethynyl-4-hexylbenzene (2) (550 mg, 2.77 mmol), 4,10-dibromoanthanthrone (515 mg, 1.11 mmol), dichlorobis(triphenylphosphine)palladium(II) (39 mg, 0.057 mmol), and copper(I) iodide (8 mg, 0.044 mmol). The flask was flushed three times using a vacuum/nitrogen cycle. Diisopropylamine (2 mL) and *o*-dichlorobenzene (15 mL) were deaerated with a continuous flow of nitrogen for 10 min and then transferred via syringe to the reaction flask. The solution was heated to 90 °C for 3 h. Once cooled, the reaction mixture was poured into MeOH (100 mL). The precipitate was recovered via filtration, and the crude residue was purified by silica gel column chromatography ($\text{CHCl}_3/\text{AcOEt}$ from 100:0 to 95:5 v/v) to afford compound 5 as a purple solid (400 mg, 53%). Mp: 235–238 °C. ^1H NMR (500 MHz, CDCl_3): δ 8.69 (m, 4H), 8.47 (s, 2H), 7.87–7.81 (m, 2H), 7.57 (d, J = 7.5 Hz, 4H), 7.91 (d, J = 7.9 Hz, 4H), 2.67 (t, J = 7.8 Hz, 4H), 1.70–1.63 (m, 4H), 1.42–1.29 (m, 12H), 0.92 (t, J = 6.4 Hz, 6H). ^{13}C NMR (125 MHz, CDCl_3): δ 182.2, 144.5, 133.8, 133.7, 131.9, 131.2, 129.3, 129.2, 128.7, 128.7, 128.1, 127.4, 126.9, 124.4, 119.7, 98.4, 86.1, 36.1, 31.7, 31.3, 29.0, 22.6, 14.1. HRMS (APPI+): calcd for $\text{C}_{50}\text{H}_{43}\text{O}_2$ ($M + \text{H}$)⁺ 675.3258, found 675.3266.

4,10-Bis((5-octyl-2-thienyl)ethynyl)anthanthrone (6). A dry flask under nitrogen was charged with 2-ethynyl-5-octylthiophene (4) (522 mg, 2.37 mmol), 4,10-dibromoanthanthrone (500 mg, 1.08 mmol), dichlorobis(triphenylphosphine)palladium(II) (38 mg, 0.054 mmol), and copper(I) iodide (10 mg, 0.054 mmol), and the flask was flushed three times using a vacuum/nitrogen cycle. Diisopropylamine (2 mL) and *o*-dichlorobenzene (10 mL) were deaerated with a continuous flow of nitrogen for 10 min and then transferred via syringe to the reaction flask. The solution was heated to 90 °C for 4 h. Once cooled, the mixture was

poured into MeOH (100 mL). The precipitate was recovered via filtration, and the crude residue was purified by silica gel column chromatography (CHCl_3) to afford compound **6** as a blue solid (99 mg, 12%). ^1H NMR analysis was performed at 50 °C because of peak broadening and poor solubility at room temperature. Acquisition of the ^{13}C NMR spectrum proved unsuccessful because of the poor solubility and precipitation of the product during the course of the acquisition. Mp: 165–170 °C. ^1H NMR (500 MHz, 50 °C, CDCl_3): δ 8.69 (d, J = 7.0 Hz, 2H), 8.64 (d, J = 8.3 Hz, 2H), 8.50 (s, 2H), 7.89–7.83 (m, 2H), 7.29 (d, J = 3.4 Hz, 2H), 6.78 (d, J = 3.0 Hz, 2H), 2.88 (t, J = 7.8 Hz, 4H), 1.80–1.72 (m, 4H), 1.51–1.28 (m, 24H), 0.93 (t, J = 7.0 Hz, 6H). HRMS (APPI+): calcd for $\text{C}_{50}\text{H}_{47}\text{O}_2\text{S}_2$ ($M + \text{H}$)⁺ 743.3012, found 743.3024.

4,6,10,12-Tetrakis((4-hexylphenyl)ethynyl)anthanthrene (7).

A dry flask under nitrogen was charged with 1-ethynyl-4-hexylbenzene (409 mg, 2.07 mmol) and anhydrous THF (20 mL) and cooled to 0 °C. A solution of *n*-butyllithium in hexanes (2.5 M, 0.83 mL, 2.07 mmol) was added dropwise over 5 min. After 20 min at this temperature, compound **5** (280 mg, 0.414 mmol) was added in a single portion under a positive nitrogen pressure, and the reaction mixture was warmed to room temperature overnight. Tin(II) chloride dihydrate (400 mg, 1.78 mmol) dissolved in aqueous HCl (10% v/v, 4 mL) was added dropwise to the reaction mixture. After 20 min, the mixture was poured into MeOH (100 mL). The precipitate was recovered via filtration, and the crude residue was dissolved in CHCl_3 with silica gel (3 g) and evaporated under reduced pressure. The crude product adsorbed on silica gel was purified by silica gel column chromatography (toluene/hexanes 20:80 v/v) to afford compound **7** as a purple solid (105 mg, 25%). Mp: 200–204 °C. ^1H NMR (500 MHz, CDCl_3): δ 8.86 (d, J = 8.2 Hz, 2H), 8.73 (s, 2H), 8.62 (d, J = 7.0 Hz, 2H), 8.06 (t, J = 7.8 Hz, 2H), 7.76 (d, J = 8.2 Hz, 4H), 7.76 (d, J = 7.8 Hz, 4H), 7.28–7.23 (m, 8H), 2.76–2.68 (m, 8H), 1.76–1.66 (m, 8H), 1.47–1.33 (m, 24H), 0.97–0.92 (m, 12H). ^{13}C NMR (125 MHz, CDCl_3): δ 143.2 (2C), 132.0, 131.9, 130.6, 130.0, 129.8, 129.7, 128.5 (2C), 126.1, 125.7, 124.2, 121.7, 121.4, 121.1, 121.0, 119.7, 116.5, 102.5, 95.0, 87.9, 86.5, 36.2, 36.1, 31.9, 31.8, 31.4 (2C), 29.2, 29.1, 22.7 (2C), 14.2 (2C). HRMS (APPI+): calcd for $\text{C}_{78}\text{H}_{77}$ ($M + \text{H}$)⁺ 1013.6020, found 1013.5984.

4,10-Dibromo-6,12-bis((triisopropylsilyl)ethynyl)anthanthrene (9).

A dry flask under nitrogen was charged with (triisopropylsilyl)-acetylene (1.96 g, 10.77 mmol) and anhydrous THF (45 mL) and cooled to 0 °C. A solution of *n*-butyllithium in hexanes (2.4 M, 4.5 mL, 10.77 mmol) was added dropwise over 10 min. After 20 min at this temperature, 4,10-dibromoanthanthrene (1.00 g, 2.15 mmol) was added in one portion under a positive nitrogen pressure. The reaction mixture was allowed to warm to room temperature overnight. A solution of tin(II) chloride dihydrate (2.8 g, 9.26 mmol) in aqueous HCl (50% v/v, 2.5 mL) was added dropwise, and the resulting mixture was stirred for 20 min and then poured into MeOH (100 mL). The precipitate was recovered via filtration, and the residue was dissolved in warm CHCl_3 and filtered again. The filtrate was evaporated under reduced pressure, and the crude product was recrystallized from hexanes (at room temperature) to afford compound **9** as a red solid (830 mg, 48%). Mp: 150–155 °C. ^1H NMR (500 MHz, CDCl_3): δ 9.21 (s, 2H), 9.18 (d, J = 8.2 Hz, 2H), 8.77 (d, J = 7 Hz, 2H), 8.36–8.31 (m, 2H), 1.44–1.33 (m, 42H). ^{13}C NMR (125 MHz, CDCl_3): δ 132.5, 130.7, 130.5, 130.0, 127.4, 127.0, 126.3, 125.5, 122.9, 120.8, 116.9, 105.6, 103.2, 19.0, 11.6. HRMS (APPI+): calcd for $\text{C}_{44}\text{H}_{51}\text{Br}_2\text{Si}_2$ ($M + \text{H}$)⁺ 793.1891, found 793.1878.

4,6,10,12-Tetrakis(5-octyl-2-thienyl)anthanthrene (11).

A dry flask under nitrogen was charged with 2-octylthiophene (113 mg, 0.58 mmol) and anhydrous THF (3 mL) and cooled to 0 °C. A solution of *n*-butyllithium in hexanes (2.5 M, 0.23 mL, 0.58 mmol) was added dropwise over 5 min. After 20 min at this temperature, this solution was transferred via cannula to a flask containing 4,10-bis(5-octyl-2-thienyl)anthanthrene (**10**) (100 mg, 0.14 mmol) and anhydrous THF (10 mL) at 0 °C. After 1 h at this temperature, a solution of tin(II) chloride dihydrate (400 mg, 1.78 mmol) in aqueous HCl (10% v/v, 4 mL) was added dropwise, and the resulting mixture was allowed to warm to room temperature over 1 h. Water was added to the reaction mixture, and the organic layer was extracted twice with

CH_2Cl_2 . The organic layer was dried with MgSO_4 , and the solvent was evaporated under reduced pressure. The crude product was purified by silica gel column chromatography (CH_2Cl_2 /hexanes 10:90 v/v) followed by recrystallization in hexanes (at ca. –15 °C) to afford compound **11** as a yellow solid (57 mg, 39%). Mp: 145–150 °C. ^1H NMR (500 MHz, CDCl_3): δ 8.68 (d, J = 7.5 Hz, 2H), 8.52 (d, J = 8.3 Hz, 2H), 8.28 (s, 2H), 8.12–8.06 (m, 2H), 7.28–7.26 (m, 4H), 7.19 (d, J = 3.2 Hz, 2H), 7.05 (d, J = 2.6 Hz, 2H), 3.02 (t, J = 7.3 Hz, 4H), 2.93 (t, J = 7.3 Hz, 4H), 1.91–1.77 (m, 8H), 1.56–1.28 (m, 40H), 0.95–0.88 (m, 12H). ^{13}C NMR (125 MHz, CDCl_3): δ 147.7, 146.5, 139.6, 136.4, 133.3, 131.8, 130.4, 129.9, 129.7, 128.8, 127.9, 127.4, 125.9, 125.9, 124.2, 124.2, 123.6, 123.1, 121.9, 32.0, 31.9, 31.8, 31.7, 30.4, 30.3, 29.7, 29.4 (3C), 29.3 (2C), 22.7 (2C), 14.2, 14.1. HRMS (APPI+): calcd for $\text{C}_{70}\text{H}_{85}\text{S}_4$ ($M + \text{H}$)⁺ 1053.5529, found 1053.5534.

2-(2-Ethylhexylthio)thiophene (12). A dry flask under nitrogen was charged with thiophene (6.00 g, 71.4 mmol) and anhydrous THF (45 mL) and cooled to 0 °C. A solution of *n*-butyllithium in hexanes (2.5 M, 28.5 mL, 71.4 mmol) was added dropwise over 10 min. After 20 min at this temperature, the reaction mixture was cooled to –78 °C using a dry ice/acetone bath, and sulfur (2.29 g, 71.4 mmol) was added in a single portion under a positive nitrogen pressure. After 30 min at –78 °C, the solution was allowed to warm to room temperature and stirred for 3 h. 2-Ethylhexyl bromide (13.78 g, 71.4 mL) was added in three portions, and the reaction mixture was stirred overnight at room temperature. Water and hexanes were added to the reaction mixture. Diluted HCl was added to break the emulsion, and the aqueous layer was extracted three times with hexanes. The organic layer was dried with MgSO_4 , and the solvent was evaporated under reduced pressure. The crude product was purified by silica gel column chromatography (hexanes) to afford compound **12** as a colorless oil (12.2 g, 80%). ^1H NMR (400 MHz, CDCl_3): δ 7.31–7.28 (m, 1H), 7.09–7.06 (m, 1H), 6.96–6.93 (m, 1H), 2.80 (d, J = 6.5 Hz, 2H), 1.56–1.18 (m, 9H), 0.91–0.80 (m, 6H). ^{13}C NMR (100 MHz, CDCl_3): δ 135.9, 132.6, 128.5, 127.4, 43.7, 38.9, 32.0, 28.7, 25.2, 22.9, 14.1, 10.6, 29.3, 29.2, 29.0, 22.7, 14.1. HRMS (APPI+): calcd for $\text{C}_{12}\text{H}_{21}\text{S}_2$ ($M + \text{H}$)⁺ 229.1079, found 229.1084.

2-Bromo-5-(2-ethylhexylthio)thiophene (13). A dry flask under nitrogen was charged with 2-(2-ethylhexylthio)thiophene (4.00 g, 17.5 mmol) and anhydrous DMF (30 mL), and *N*-bromosuccinimide (3.10 g, 17.5 mmol) was added portionwise followed by sonication for 10 min. Water and hexanes were added to the reaction mixture, and the organic layer was washed three times with water. The organic layer was dried with MgSO_4 , and the solvent was evaporated under reduced pressure to afford compound **13** as a colorless oil (5.17 g, 96%). ^1H NMR (400 MHz, CDCl_3): δ 6.90 (d, J = 3.8 Hz, 1H), 6.87 (d, J = 3.6 Hz, 1H), 2.77 (d, J = 6.2 Hz, 2H), 1.56–1.18 (m, 9H), 0.91–0.80 (m, 6H). ^{13}C NMR (100 MHz, CDCl_3): δ 137.2, 133.6, 130.3, 113.4, 43.8, 38.9, 31.9, 28.6, 25.1, 22.9, 14.1, 10.6. HRMS (APPI+): calcd for $\text{C}_{12}\text{H}_{19}\text{BrS}_2$ ($M + \text{H}$)⁺ 306.0106, found 306.0101.

2-Bromo-5-(2-ethylhexylsulfonyl)thiophene (14). A dry flask under nitrogen was charged with 2-bromo-5-(2-ethylhexylthio)thiophene (2 g, 6.50 mmol) and anhydrous DMF (80 mL). 3-Chloroperoxybenzoic acid (77% purity, 3.65 g, 16.27 mmol) was added in a single portion, and the solution was stirred overnight at room temperature. Dilute aqueous NaOH, hexanes, and AcOEt were added to the reaction mixture, and the organic layer was washed three times with dilute aqueous NaOH. The organic layer was dried with MgSO_4 , and the solvent was evaporated under reduced pressure to afford compound **14** as a colorless oil (1.599 g, 72%). ^1H NMR (400 MHz, CDCl_3): δ 7.44 (d, J = 4.0 Hz, 1H), 7.13 (d, J = 4.0 Hz, 1H), 3.11 (d, J = 5.8 Hz, 2H), 2.00–1.92 (m, 1H), 1.53–1.37 (m, 4H), 1.30–1.16 (m, 4H), 0.90–0.82 (m, 6H). ^{13}C NMR (100 MHz, CDCl_3): δ 142.0, 133.9, 130.8, 121.7, 61.3, 34.7, 32.3, 28.1, 25.6, 22.6, 14.0, 10.2, 29.3, 29.2, 29.0, 22.6, 14.1. HRMS (APPI+): calcd for $\text{C}_{12}\text{H}_{20}\text{BrO}_2\text{S}_2$ ($M + \text{H}$)⁺ 339.0083, found 339.0086.

4,10-Bis((5-octyl-2-thienyl)ethynyl)-6,12-bis((triisopropylsilyl)ethynyl)anthanthrene (15). A dry flask under nitrogen was charged with 2-ethynyl-5-octylthiophene (**4**) (522 mg, 2.37 mmol), compound **9** (200 mg, 0.252 mmol), dichlorobis(triphenylphosphine)palladium(II) (8.8 mg, 0.013 mmol), and copper(I) iodide (2.4 mg, 0.013 mmol).

The flask was flushed three times using a vacuum/nitrogen cycle. Diisopropylamine (1 mL) and THF (10 mL) were deaerated with a continuous flow of nitrogen for 10 min and transferred via syringe to the reaction flask. The solution was heated to 65 °C overnight. Once cooled, the mixture was poured into MeOH (100 mL). The precipitate was recovered via filtration and recrystallized from CHCl₃ (25 mL at ca. –15 °C) to afford compound **15** as red needles (199 mg, 74%). Mp: 190–195 °C. ¹H NMR (500 MHz, CDCl₃): δ 9.15 (d, *J* = 7.9 Hz, 2H), 9.10 (s, 2H), 8.81 (d, *J* = 7.1 Hz, 2H), 8.33–8.29 (m, 2H), 7.31 (d, *J* = 3.6 Hz, 2H), 6.79 (d, *J* = 3.3 Hz, 2H), 2.88 (t, *J* = 7.5 Hz, 4H), 1.78–1.72 (m, 4H), 1.46–1.28 (m, 62H), 0.91 (t, *J* = 6.5 Hz, 6H). ¹³C NMR (125 MHz, CDCl₃): δ 149.2, 132.6, 131.9, 131.4, 131.0, 130.1, 127.1, 126.4, 124.7, 124.5, 122.6, 122.4, 121.0, 120.5, 117.3, 105.4, 103.6, 91.1, 88.9, 31.9, 31.6, 30.4, 29.4, 29.3, 29.1, 22.7, 19.0, 14.1, 11.7. HRMS (APPI+): calcd for C₇₂H₈₉S₂Si₂ (M + H)⁺ 1073.5939, found 1073.5947.

General Procedure for TIPS-Acetylene Deprotection with TBAF (Procedure A). To a solution of the bis(TIPS-acetylene) compound in THF (5–10 mL) containing water (3 drops) under nitrogen was added a solution of tetrabutylammonium fluoride in THF (1 M, 3 equiv). The reaction was monitored using TLC. After 1 h, MeOH (10–20 mL) was added, and the crude bis(ethynyl) product was recovered by filtration in over 90% yield and used in the next step without further purification.

General Procedure for Twofold Sonogashira Coupling Using the Pd₂(dba)₃/tBu₃PBHF₄ Catalyst (Procedure B). In order to ensure proper stoichiometry, a mixture of catalysts was prepared by grinding tris(dibenzylideneacetone)dipalladium(0)/tri-*tert*-butylphosphonium tetrafluoroborate/copper(I) iodide [Pd₂(dba)₃/tBu₃PBHF₄/CuI] in a ratio of 1:4:1 (2 equiv of phosphine per Pd, total MW 2455 g/mol) in a mortar and pestle and stored in a desiccator.

A dry flask under nitrogen was charged with bis(ethynyl)-anthanthrene compound (100–200 mg, 1 equiv), aryl bromide (2–3 equiv), and the Pd₂(dba)₃/tBu₃PBHF₄/CuI mixture (0.05 equiv relative to the anthanthrene compound), and the flask was flushed three times using a vacuum/nitrogen cycle. Diisopropylamine (1 mL) and toluene (5 mL) were deaerated with a continuous flow of nitrogen for 10 min and transferred via syringe to the reaction flask, and the mixture was heated to 75 °C overnight. Once cooled, the mixture was poured into MeOH (100 mL). The precipitate was recovered via filtration and purified according to the specified procedure for each compound.

4,6,10,12-Tetrakis((5-octyl-2-thienyl)ethynyl)anthanthrene (16). Compound **15** (170 mg, 0.158 mmol) was deprotected according to procedure A to afford the terminal alkyne (112 mg, 93%). The Sonogashira coupling was performed according to procedure B using the crude product (100 mg, 0.131 mmol) and 5-bromo-2-octylthiophene (109 mg, 0.393 mmol). The crude product was purified by silica gel column chromatography (toluene/hexanes 15:85 to 100:0 v/v) followed by trituration with hot acetone to afford compound **16** as a black solid (121 mg, 80%). Mp: 144–148 °C. ¹H NMR (400 MHz, CDCl₃): δ 8.73 (d, *J* = 8.0 Hz, 2H), 8.50 (d, *J* = 7.6 Hz, 2H), 8.43 (s, 2H), 8.07–8.01 (m, 2H), 8.37 (d, *J* = 3.4 Hz, 2H), 7.37 (d, *J* = 3.4 Hz, 2H), 7.31 (d, *J* = 3.5 Hz, 2H), 6.80 (d, *J* = 3.2 Hz, 2H), 6.77 (d, *J* = 3.4 Hz, 2H), 2.93–2.84 (m, 8H), 1.85–1.72 (m, 8H), 1.52–1.23 (m, 40H), 0.95–0.90 (m, 12H). ¹³C NMR (125 MHz, CDCl₃): δ 148.9, 148.6, 132.5 (2C), 130.2, 129.8 (2C), 129.6, 126.4 (2C), 125.9, 124.5, 124.3, 121.6, 121.5, 121.1, 121.0, 119.9, 116.4, 96.2, 91.5, 90.3, 88.8, 32.0, 31.9, 31.7 (2C), 30.5, 30.4, 29.5 (2C), 29.4, 29.3 (3C), 22.74, 14.18. HRMS (APPI+): calcd for C₇₈H₈₅S₄ (M + H)⁺ 1149.5529, found 1149.5550.

4,10-Bis(5-octyl-2-thienyl)-6,12-bis((triisopropylsilyl)ethynyl)anthanthrene (17). A dry flask under nitrogen was charged 2-octylthiophene (198 mg, 1.00 mmol) and dry THF (5 mL). The mixture was cooled to –78 °C, and *n*-butyllithium (2.5 M in hexane, 1.72 mL, 4.3 mmol) was added dropwise. The mixture was stirred for 60 min before the addition of Bu₃SnCl (352 mg, 1.08 mmol) dropwise. The mixture was warmed to room temperature over 1 h. A second dry flask under nitrogen was charged with compound **9** (200 mg, 0.252 mmol), dichlorobis(triphenylphosphine)palladium(II) (9 mg, 0.013 mmol), and toluene (10 mL). The mixture was degassed with a flow of nitrogen for 10 min, and the stannyl solution was

transferred with a syringe. The resulting mixture was heated at 90 °C overnight. Once cooled, the mixture was poured into MeOH (100 mL). The precipitate was recovered via filtration, and the residue was purified by silica gel column chromatography (CH₂Cl₂/hexanes 0:100 to 4:96 v/v) followed by recrystallization in hexanes (ca. 15 mL at –15 °C) to afford compound **17** as an orange solid (194 mg, 75%). Mp: 170–173 °C. ¹H NMR (500 MHz, CDCl₃): δ 9.21 (d, *J* = 8.14 Hz, 2H), 8.98 (s, 2H), 8.89 (d, *J* = 7.3 Hz, 2H), 8.30–8.26 (m, 2H), 7.43 (d, *J* = 3.4 Hz, 2H), 6.99 (d, *J* = 3.4 Hz, 2H), 2.99 (t, *J* = 7.5 Hz, 4H), 1.88–1.81 (m, 4H), 1.54–1.29 (m, 62H), 0.98–0.89 (m, 6H). ¹³C NMR (125 MHz, CDCl₃): δ 146.8, 139.2, 134.4, 132.2, 131.4, 130.4, 128.0, 127.6, 126.8, 125.9, 124.6, 124.4, 122.9, 121.2, 117.3, 104.7, 104.1, 32.0 (2C), 30.4, 29.5, 29.3 (2C), 22.7, 19.1, 14.2, 11.6. HRMS (APPI+): calcd for C₆₈H₈₉S₂Si₂ (M + H)⁺ 1025.5939, found 1025.5951.

4,10-Bis(5-octyl-2-thienyl)-6,12-bis((5-octyl-2-thienyl)ethynyl)anthanthrene (18). Compound **17** (170 mg, 0.166 mmol) was deprotected according to procedure A, except that CH₂Cl₂ (20 mL) was used instead of THF, to afford the terminal bis(alkyne) (109 mg, 93%). The Sonogashira coupling was performed according to procedure B using the crude bis(acetylene) product (90 mg, 0.126 mmol) and 5-bromo-2-octylthiophene (109 mg, 0.393 mmol). The crude product was purified by silica gel column chromatography (CH₂Cl₂/hexanes 10:90 v/v) followed by recrystallization in CH₂Cl₂/hexanes to afford compound **18** as a golden solid (122 mg, 87%). Mp: 175–180 °C. ¹H NMR (500 MHz, CDCl₃): δ 8.86 (d, *J* = 7.3 Hz, 2H), 8.66 (d, *J* = 7.3 Hz, 2H), 8.63 (s, 2H), 8.10–8.04 (m, 2H), 7.38 (d, *J* = 3.3 Hz, 2H), 7.34 (d, *J* = 3.4 Hz, 2H), 6.97 (d, *J* = 2.9 Hz, 2H), 6.81 (d, *J* = 3.2 Hz, 2H), 2.99 (t, *J* = 7.5 Hz, 4H), 2.90 (t, *J* = 7.7 Hz, 4H), 1.90–1.74 (m, 8H), 1.57–1.27 (m, 40H), 0.96–0.88 (m, 12H). ¹³C NMR (125 MHz, CDCl₃): δ 149.0, 146.6, 139.4, 133.9, 132.3, 130.7, 130.4, 130.2, 127.7, 127.7, 126.3, 125.6, 124.5, 124.4, 124.3, 122.4, 121.1, 120.7, 116.5, 95.9, 90.8, 32.0, 31.9 (2C), 31.7, 30.5, 30.4, 29.5, 29.4 (3C), 29.3, 29.2, 22.8, 22.7, 14.2 (2C). HRMS (APPI+): calcd for C₇₄H₈₅S₄ (M + H)⁺ 1101.5529, found 1101.5557.

4,10-Bis((trimethylsilyl)ethynyl)-6,12-bis((triisopropylsilyl)ethynyl)anthanthrene (19). A dry flask under nitrogen was charged with compound **9** (400 mg, 0.503 mmol), dichlorobis(triphenylphosphine)palladium(II) (18 mg, 0.025 mmol), and copper(I) iodide (4.8 mg, 0.025 mmol). The flask was flushed three times with a vacuum/nitrogen cycle. Diisopropylamine (2 mL) and THF (10 mL) were deaerated with a continuous flow of nitrogen for 10 min and transferred via syringe to the reaction flask, and (trimethylsilyl)-acetylene (198 mg, 2.01 mmol) was added. The mixture was heated to 60 °C overnight. Once the mixture was cooled, a saturated NH₄Cl solution was added, and the aqueous layer was extracted twice with CH₂Cl₂. The organic layer was dried with MgSO₄, and the solvent was evaporated under reduced pressure. The crude product was purified by silica gel column chromatography (CH₂Cl₂/hexanes 0:100 to 5:95 v/v) to afford compound **19** as a red solid (380 mg, 91%). Mp: 190–195 °C. ¹H NMR (500 MHz, CDCl₃): δ 9.16–9.12 (m, 4H), 8.81 (d, *J* = 7.40 Hz, 2H), 8.33–8.29 (m, 2H), 1.42–1.25 (m, 42H), 0.43 (s, 18H). ¹³C NMR (125 MHz, CDCl₃): δ 132.9, 131.8, 130.9, 130.3, 127.1, 126.4, 124.9, 122.5 (2C), 121.1, 117.5, 105.4, 103.6, 103.2, 100.4, 19.0, 11.7, 0.1. HRMS (APPI+): calcd for C₅₄H₆₉Si₄ (M + H)⁺ 829.4471, found 829.4462.

4,10-Bis((5-(2,5-dioctyl-6-(thiophen-2-yl)-1,4(2H,5H)-dioxopyrrolo[3,4-*c*]pyrrol-3-yl)-2-thienyl)ethynyl)-6,12-bis((triisopropylsilyl)ethynyl)anthanthrene (20). To a solution of bis(TMS-acetylene) compound **19** (300 mg, 0.363 mmol) in THF (10 mL) and MeOH (10 mL) containing water (3 drops) under nitrogen was added K₂CO₃ (150 mg, 1.09 mmol). After 1 h, MeOH (20 mL) was added, and the crude product was recovered via filtration after washing with 1% aqueous HCl and MeOH to afford the bis(ethynyl) compound (190 mg, 77% yield), which was used for the synthesis of compounds **20** and **21**. The Sonogashira coupling was performed according to procedure B using the crude bis(ethynyl) compound (40 mg, 0.058 mmol) and 3-(5-bromothiophen-2-yl)-2,5-dioctyl-6-(thiophen-2-yl)pyrrolo[3,4-*c*]pyrrole-1,4(2H,5H)-dione (**5-Br-DPP**) (70 mg, 0.116 mmol). The crude product was purified by silica gel column chromatography (CHCl₃/AcOEt 100:0 to 99:1 v/v) to afford compound **20** as a dark solid (49 mg, 49%). Mp: >260 °C. ¹H NMR

(500 MHz, CDCl_3): δ 9.01 (d, J = 7.8 Hz, 2H), 8.83 (br s, 4H), 8.65 (d, J = 7.2 Hz, 2H), 8.56 (s, 2H), 8.35–8.31 (m, 2H), 7.49 (d, J = 4.8 Hz, 2H), 7.35 (d, J = 3.6 Hz, 2H), 7.14 (t, J = 3.8 Hz, 2H), 4.01–3.89 (m, 8H), 1.76–1.25 (m, 90H), 0.94–0.85 (m, 12H). ^{13}C NMR (125 MHz, CDCl_3): δ 160.5 (2C), 139.5, 138.1, 135.7, 135.6, 133.5, 131.9, 131.0, 130.8, 130.6, 130.4, 129.7, 129.1, 128.5 (2C), 128.3, 127.3 (2C), 126.5, 124.4, 121.4, 117.2, 108.0, 107.4, 105.4, 103.5, 96.7, 87.9, 31.9, 31.8, 29.5, 29.4, 29.3 (2C), 27.1, 27.0, 22.7 (2C), 19.2, 14.1 (2C), 11.8. HRMS (APPI+): calcd for $\text{C}_{108}\text{H}_{129}\text{N}_4\text{O}_4\text{S}_4\text{Si}_2$ ($\text{M} + \text{H}$)⁺ 1730.8469, found 1730.8477.

4,10-Bis((5-(2-ethylhexylthio)-2-thienyl)ethynyl)-6,12-bis((triisopropylsilyl)ethynyl)anthanthrene (21). The Sonogashira coupling was performed according to procedure B using the crude 4,10-bis(ethynyl)-6,12-bis((triisopropylsilyl)ethynyl)anthanthrene prepared in the synthesis of compound **20** (80 mg, 0.117 mmol) and compound **13** (108 mg, 0.350 mmol). The crude product was purified by silica gel column chromatography (CH_2Cl_2 /hexanes 5:95 v/v) to afford compound **21** as an orange solid (115 mg, 87%). *Acetone was added during the last evaporation step to obtain a powdery solid.* Mp: 100–103 °C. ^1H NMR (500 MHz, CDCl_3): δ 9.06 (d, J = 8.2 Hz, 2H), 8.90 (s, 2H), 8.75 (d, J = 7.6 Hz, 2H), 8.32–8.26 (m, 2H), 7.31 (d, J = 2.7 Hz, 2H), 7.06 (d, J = 2.5 Hz, 2H), 2.96 (d, J = 5.9 Hz, 4H), 1.70–1.25 (m, 60H), 1.00–0.89 (m, 12H). ^{13}C NMR (125 MHz, CDCl_3): δ 139.2, 132.7, 131.8, 131.6, 131.5, 130.7, 129.7, 127.1, 126.4, 125.4, 124.6, 122.1, 122.1, 120.7, 117.2, 105.3, 103.6, 92.5, 87.9, 43.4, 39.2, 32.1, 28.8, 25.3, 23.0, 19.1, 14.2, 11.7, 10.8. HRMS (APPI+): calcd for $\text{C}_{72}\text{H}_{89}\text{S}_4\text{Si}_2$ ($\text{M} + \text{H}$)⁺ 1137.5380, found 1137.5374.

4,10-Bis((5-(2-ethylhexylthio)-2-thienyl)ethynyl)-6,12-bis((5-(2-ethylhexylsulfonyl)-2-thienyl)ethynyl)anthanthrene (22). Compound **21** (75 mg, 0.066 mmol) was deprotected according to procedure A to afford the bis(acetylene) (52 mg, 96%). The Sonogashira coupling was performed according to procedure B using the crude bis(acetylene) product (70 mg, 0.084 mmol) and compound **14** (71 mg, 0.212 mmol). The crude product was purified by silica gel column chromatography (CH_2Cl_2 /AcOEt 100:0 to 99:1 v/v) followed by recrystallization in CH_2Cl_2 /hexanes to afford compound **22** as a red solid (104 mg, 91%). Mp: 235–240 °C. ^1H NMR (400 MHz, CDCl_3): δ 8.32 (d, J = 8.6 Hz, 2H) 8.23 (d, J = 7.6 Hz, 2H), 7.89–7.81 (m, 4H), 7.67 (d, J = 3.7 Hz, 2H), 7.40 (d, J = 3.9 Hz, 2H), 7.31 (d, J = 3.5 Hz, 2H), 7.06 (d, J = 3.5 Hz, 2H), 3.30 (d, J = 5.7 Hz, 2H), 3.01 (d, J = 6.2 Hz, 2H), 2.21–2.12 (m, 2H), 1.72–1.21 (m, 34H), 1.05–0.78 (m, 24H). ^{13}C NMR (125 MHz, CDCl_3): δ 141.9, 139.7, 133.7, 133.1, 132.1, 131.4, 131.3, 129.1, 128.5, 128.4, 128.3, 126.1, 125.0, 124.8, 124.4, 121.3, 119.8, 118.6, 114.2, 94.1, 93.4, 92.0, 88.6, 61.5, 43.4, 39.2, 34.8, 32.5, 32.2, 28.8, 28.3, 25.8, 25.4, 23.1, 22.9, 14.2 (2C), 10.9, 10.4. HRMS (APPI+): calcd for $\text{C}_{78}\text{H}_{85}\text{O}_4\text{S}_8$ ($\text{M} + \text{H}$)⁺ 1342.4247, found 1342.4127.

4,10-Bis((triisopropylsilyl)ethynyl)-6,12-bis((trimethylsilyl)ethynyl)anthanthrene (24). A dry flask under nitrogen was charged with (trimethylsilyl)acetylene (736 mg, 7.49 mmol) and anhydrous THF (15 mL) and cooled to 0 °C. A solution of *n*-butyllithium in hexanes (2.5 M, 3.0 mL, 7.49 mmol) was added dropwise over 10 min. After 20 min at this temperature, 4,10-bis((triisopropylsilyl)ethynyl)anthanthrene (**23**) (500 mg, 0.75 mmol) was added in one portion under a positive nitrogen pressure. The reaction mixture was allowed to warm to room temperature overnight. A solution of tin(II) chloride dihydrate (974 mg, 3.22 mmol) in aqueous HCl (50% v/v, 2 mL) was added dropwise, and the resulting mixture was stirred for 20 min and then poured into MeOH (100 mL). The precipitate was recovered via filtration, and the residue was purified by silica gel column chromatography (CH_2Cl_2 /hexanes 0:100 to 5:95 v/v) to afford compound **24** as a red solid (480 mg, 77%). Mp: >260 °C. ^1H NMR (500 MHz, CDCl_3): δ 9.11 (d, J = 8.2 Hz, 2H), 9.02 (s, 2H), 8.36 (d, J = 7.4 Hz, 2H), 8.33–8.29 (m, 2H), 1.37–1.26 (m, 42H), 0.53 (s, 18H). ^{13}C NMR (125 MHz, CDCl_3): δ 132.5, 131.7, 130.6, 130.4, 127.1, 126.4, 124.9, 122.9, 122.3, 121.1, 117.0, 108.6, 105.3, 101.8, 97.1, 18.9, 11.5, 0.2. HRMS (APPI+): calcd for $\text{C}_{54}\text{H}_{69}\text{Si}_4$ ($\text{M} + \text{H}$)⁺ 829.4471, found 829.4443.

4,10-Bis((triisopropylsilyl)ethynyl)-6,12-bis((5-(2,5-dioctyl-6-(thiophen-2-yl)-1,4(2H,5H)-dioxopyrrolo[3,4-c]pyrrol-3-yl)-2-thienyl)ethynyl)anthanthrene (25). To a solution of bis(TMS-acetylene) compound **24** (300 mg, 0.362) in THF (15 mL) and MeOH (10 mL) containing water (3 drops) under nitrogen was added

K_2CO_3 (150 mg, 1.09 mmol). After 1 h, MeOH (20 mL) was added, and the crude product was recovered via filtration and washed with 1% aqueous HCl and MeOH to afford the bis(acetylene) compound (244 mg, 98% yield), which was used for the synthesis of compounds **25** and **26**. The Sonogashira coupling was performed according to procedure B using the crude bis(acetylene) product (40 mg, 0.058 mmol) and 3-(5-bromothiophen-2-yl)-2,5-dioctyl-6-(thiophen-2-yl)-pyrrolo[3,4-c]pyrrole-1,4(2H,5H)-dione (**5-Br-DPP**) (70 mg, 0.116 mmol). The crude product was purified by silica gel column chromatography (CHCl_3) to afford compound **20** as a blue solid (62 mg, 62%). Mp: >260 °C. ^1H NMR (500 MHz, CDCl_3): δ 9.08 (br s, 2H), 8.90 (br s, 2H), 8.84 (d, J = 7.2 Hz, 2H), 8.45–8.40 (m, 2H), 8.30 (br s, 2H), 8.24–8.17 (m, 2H), 7.59 (d, J = 3.0 Hz, 2H), 7.46 (d, J = 4.4 Hz, 2H), 7.08 (m, 2H), 4.13–3.90 (m, 8H), 1.82–1.20 (m, 90 H), 0.96–0.75 (m, 12H). ^{13}C NMR (125 MHz, CDCl_3): δ 160.6 (2C), 139.7, 138.1, 135.8, 135.7, 133.8, 133.7, 131.4, 130.5, 129.9, 129.8, 129.2, 128.5, 128.4, 127.3, 125.8, 125.2 (2C), 122.2, 121.0 (2C), 115.6, 108.4, 107.5, 105.4, 97.2, 96.3, 96.2, 31.9 (2C), 29.5, 29.3 (3C), 27.1, 27.0, 22.7 (2C), 19.1, 14.2, 14.1, 11.7. HRMS (APPI+): calcd for $\text{C}_{108}\text{H}_{129}\text{N}_4\text{O}_4\text{S}_4\text{Si}_2$ ($\text{M} + \text{H}$)⁺ 1730.8469, found 1730.8444.

4,10-Bis((triisopropylsilyl)ethynyl)-6,12-bis((5-(2-ethylhexylthio)-2-thienyl)ethynyl)anthanthrene (26). The Sonogashira coupling was performed according to procedure B using the crude 4,10-bis((triisopropylsilyl)ethynyl)-6,12-bis(ethynyl)anthanthrene prepared in the synthesis of compound **25** (100 mg, 0.146 mmol) and compound **13** (134 mg, 0.438 mmol). The crude product was purified by silica gel column chromatography (CH_2Cl_2 /hexanes 5:95 v/v) to afford compound **26** as a purple solid (147 mg, 94%). Mp: 188–192 °C. ^1H NMR (400 MHz, CDCl_3): δ 8.77 (d, J = 8.2 Hz, 2H), 8.36–8.32 (m, 4H), 8.08–8.02 (m, 2H), 7.30 (d, J = 3.5 Hz, 2H), 7.02 (d, J = 3.7 Hz, 2H), 1.74–1.21 (m, 60H), 1.03–0.94 (m, 12H). ^{13}C NMR (100 MHz, CDCl_3): δ 139.1, 132.4, 131.6, 131.4, 129.7, 129.3, 126.6, 125.7 (2C), 124.6, 121.7, 121.0, 119.5, 115.9, 105.5, 96.3, 95.5, 91.7, 43.4, 39.1, 32.1, 28.8, 25.3, 23.0, 19.0, 14.1, 11.6, 10.8. HRMS (APPI+): calcd for $\text{C}_{72}\text{H}_{89}\text{S}_4\text{Si}_2$ ($\text{M} + \text{H}$)⁺ 1137.5380, found 1137.5372.

4,10-Bis((5-(2-ethylhexylsulfonyl)-2-thienyl)ethynyl)-6,12-bis((5-(2-ethylhexylthio)-2-thienyl)ethynyl)anthanthrene (27). Compound **26** (140 mg, 0.123 mmol) was deprotected according to procedure A to afford the bis(acetylene) (98 mg, 96%). The Sonogashira coupling was performed according to procedure B using the crude bis(acetylene) product (90 mg, 0.109 mmol) and compound **14** (111 mg, 0.327 mmol). The crude product was purified by silica gel column chromatography (CH_2Cl_2 /AcOEt 100:0 to 99:1 v/v) to afford compound **22** as a dark solid (46 mg, 31%). Mp: 205–210 °C. ^1H NMR (500 MHz, CDCl_3): δ 8.24 (d, J = 7.72 Hz, 2H), 8.04 (d, J = 7.1 Hz, 2H), 7.77–7.73 (m, 2H), 7.68 (s, 2H), 7.63 (d, J = 3.6 Hz, 2H), 7.32 (d, J = 3.6 Hz, 2H), 7.28–7.26 (m, 2H), 7.07 (d, J = 3.4 Hz, 2H), 3.32–3.28 (m, 4H), 3.04 (d, J = 6.5 Hz, 4H), 2.20–2.14 (m, 2H), 1.76–1.32 (m, 34H), 1.09–0.90 (m, 24H). ^{13}C NMR (125 MHz, CDCl_3): δ 141.8, 140.0, 133.5, 132.8, 132.3, 131.5 (2C), 130.6 (2C), 128.8, 128.4, 128.3, 126.1, 125.7, 125.0, 123.9, 120.6, 118.8, 116.2, 95.8, 95.6, 91.1, 86.2, 61.5, 43.4, 39.3, 34.8, 32.5, 32.2, 28.8, 28.3, 25.8, 25.4, 23.1, 22.8, 14.2, 14.1, 10.9, 10.3. HRMS (APPI+): calcd for $\text{C}_{78}\text{H}_{85}\text{O}_4\text{S}_8$ ($\text{M} + \text{H}$)⁺ 1341.4208, found 1341.4170.

■ ASSOCIATED CONTENT

■ Supporting Information

Optical and electrochemical characterizations of selected compounds, NMR spectra, and calculated coordinates and total energies. This material is available free of charge via the Internet at <http://pubs.acs.org>.

■ AUTHOR INFORMATION

Corresponding Author

*E-mail: jean-francois.morin@chm.ulaval.ca.

Notes

The authors declare no competing financial interest.

■ ACKNOWLEDGMENTS

This work was supported by NSERC through a Discovery Grant. J.-B.G. thanks the NSERC for a Ph.D. scholarship and Marc-André Courtemanche (ULaval) for assistance with the DFT calculations.

■ REFERENCES

- (1) Hückel, E. Z. *Phys.* **1931**, 70, 204–286.
- (2) Clar, E.; Schoental, R. *Polycyclic Hydrocarbons*; Academic Press: New York, 1964; Vol. 2.
- (3) Wang, C.; Dong, H.; Hu, W.; Liu, Y.; Zhu, D. *Chem. Rev.* **2012**, 112, 2208–2267.
- (4) Cheng, Y.-J.; Yang, S.-H.; Hsu, C.-S. *Chem. Rev.* **2009**, 109, 5868–5923.
- (5) Kaur, I.; Jia, W.; Kopreski, R. P.; Selvarasah, S.; Dokmeci, M. R.; Pramanik, C.; McGruer, N. E.; Miller, G. P. *J. Am. Chem. Soc.* **2008**, 130, 16274–16286.
- (6) Dong, H.; Fu, X.; Liu, J.; Wang, Z.; Hu, W. *Adv. Mater.* **2013**, 25, 6158–6183.
- (7) Takimiya, K.; Osaka, I.; Nakano, M. *Chem. Mater.* **2014**, 26, 587–593.
- (8) Mei, J.; Diao, Y.; Appleton, A. L.; Fang, L.; Bao, Z. *J. Am. Chem. Soc.* **2013**, 135, 6724–6746.
- (9) Shin, J.; Kang, N. S.; Kim, K. H.; Lee, T. W.; Jin, J.-I.; Kim, M.; Lee, K.; Ju, B. K.; Hong, J.-M.; Choi, D. H. *Chem. Commun.* **2012**, 48, 8490–8492.
- (10) Zhang, L.; Walker, B.; Liu, F.; Colella, N. S.; Mannsfeld, S. C.; Watkins, J. J.; Nguyen, T.-Q.; Briseno, A. L. *J. Mater. Chem.* **2012**, 22, 4266–4268.
- (11) Giguère, J.-B.; Verolet, Q.; Morin, J.-F. *Chem.—Eur. J.* **2013**, 19, 372–381.
- (12) Giguère, J.-B.; Morin, J.-F. *J. Org. Chem.* **2013**, 78, 12769–12778.
- (13) Roncali, J. *Macromol. Rapid Commun.* **2007**, 28, 1761–1775.
- (14) Saleh, M.; Baumgarten, M.; Mavrinskiy, A.; Schäfer, T.; Müllen, K. *Macromolecules* **2010**, 43, 137–143.
- (15) Hundertmark, T.; Littke, A. F.; Buchwald, S. L.; Fu, G. C. *Org. Lett.* **2000**, 2, 1729–1731.
- (16) Chinchilla, R.; Nájera, C. *Chem. Rev.* **2007**, 107, 874–922.
- (17) Huang, Y.; Huo, L.; Zhang, S.; Guo, X.; Han, C. C.; Li, Y.; Hou, J. *Chem. Commun.* **2011**, 47, 8904–8906.
- (18) Wu, Y.; Li, Z.; Ma, W.; Huang, Y.; Huo, L.; Guo, X.; Zhang, M.; Ade, H.; Hou, J. *Adv. Mater.* **2013**, 25, 3449–3455.
- (19) Lafleur-Lambert, A.; Rondeau-Gagné, S.; Soldera, A.; Morin, J.-F. *Tetrahedron Lett.* **2011**, 52, 5008–5011.
- (20) Würthner, F.; Kaiser, T. E.; Saha-Möller, C. R. *Angew. Chem., Int. Ed.* **2011**, 50, 3376–3410.
- (21) Gholami, M.; Tykwinski, R. R. *Chem. Rev.* **2006**, 106, 4997–5027.
- (22) Fudickar, W.; Linker, T. *J. Am. Chem. Soc.* **2012**, 134, 15071–15082.
- (23) Giessner-Prettre, C.; Pullman, B.; Borer, P. N.; Kan, L.-S.; Ts’O, P. O. P. *Biopolymers* **1976**, 15, 2277–2286.
- (24) *Binding Constants: The Measurement of Molecular Complex Stability*; Conors, K. A., Ed.; Wiley: New York, 1987.
- (25) Tobe, Y.; Utsumi, N.; Kawabata, K.; Nagano, A.; Adachi, K.; Araki, S.; Sonoda, M.; Hirose, K.; Naemura, K. *J. Am. Chem. Soc.* **2002**, 124, 5350–5364.
- (26) Floudas, G.; Pisula, W.; Chen, L.; Feng, X.; Wu, D.; Dou, X.; Müllen, K.; Yang, X. *Chem. Commun.* **2011**, 48, 702–704.
- (27) Cardona, C. M.; Li, W.; Kaifer, A. E.; Stockdale, D.; Bazan, G. C. *Adv. Mater.* **2011**, 23, 2367–2371.
- (28) Frisch, M. J.; Trucks, G. W.; Schlegel, H. B.; Scuseria, G. E.; Robb, M. A.; Cheeseman, J. R.; Scalmani, G.; Barone, V.; Mennucci, B.; Petersson, G. A.; Nakatsuji, H.; Caricato, M.; Li, X.; Hratchian, H. P.; Izmaylov, A. F.; Bloino, J.; Zheng, G.; Sonnenberg, J. L.; Hada, M.; Ehara, M.; Toyota, K.; Fukuda, R.; Hasegawa, J.; Ishida, M.; Nakajima, T.; Honda, Y.; Kitao, O.; Nakai, H.; Vreven, T.; Montgomery, J. A., Jr.; Peralta, J. E.; Ogliaro, F.; Bearpark, M.; Heyd, J. J.; Brothers, E.; Kudin, K. N.; Staroverov, V. N.; Kobayashi, R.; Normand, J.; Raghavachari, K.; Rendell, A.; Burant, J. C.; Iyengar, S. S.; Tomasi, J.; Cossi, M.; Rega, N.; Millam, J. M.; Klene, M.; Knox, J. E.; Cross, J. B.; Bakken, V.; Adamo, C.; Jaramillo, J.; Gomperts, R.; Stratmann, R. E.; Yazyev, O.; Austin, A. J.; Cammi, R.; Pomelli, C.; Ochterski, J. W.; Martin, R. L.; Morokuma, K.; Zakrzewski, V. G.; Voth, G. A.; Salvador, P.; Dannenberg, J. J.; Dapprich, S.; Daniels, A. D.; Farkas, Ö.; Foresman, J. B.; Ortiz, J. V.; Cioslowski, J.; Fox, D. J. *Gaussian 09*, revision C.01; Gaussian, Inc.: Wallingford, CT, 2010.